

# A Survey on Graph Neural Networks and Graph Transformers in Computer Vision: A Task-Oriented Perspective

Chaoqi Chen, Yushuang Wu, Qiyuan Dai, Hong-Yu Zhou, Mutian Xu,  
Sibe Yang, Xiaoguang Han, and Yizhou Yu, *Fellow, IEEE*

**Abstract**—Graph Neural Networks (GNNs) have gained momentum in graph representation learning and boosted the state of the art in a variety of areas, such as data mining (*e.g.*, social network analysis and recommender systems), computer vision (*e.g.*, object detection and point cloud learning), and natural language processing (*e.g.*, relation extraction and sequence learning), to name a few. With the emergence of Transformers in natural language processing and computer vision, graph Transformers embed a graph structure into the Transformer architecture to overcome the limitations of local neighborhood aggregation while avoiding strict structural inductive biases. In this paper, we present a comprehensive review of GNNs and graph Transformers in computer vision from a task-oriented perspective. Specifically, we divide their applications in computer vision into five categories according to the modality of input data, *i.e.*, 2D natural images, videos, 3D data, vision + language, and medical images. In each category, we further divide the applications according to a set of vision tasks. Such a task-oriented taxonomy allows us to examine how each task is tackled by different GNN-based approaches and how well these approaches perform. Based on the necessary preliminaries, we provide the definitions and challenges of the tasks, in-depth coverage of the representative approaches, as well as discussions regarding insights, limitations, and future directions.

**Index Terms**—Graph neural networks, graph Transformers, computer vision, vision and language, point clouds and meshes, medical image analysis.



## 1 INTRODUCTION

DEEP learning [1] has brought many breakthroughs to computer vision, where convolutional neural networks (CNN) take a dominant position and become the fundamental infrastructure of many modern vision systems. In particular, a number of state-of-the-art CNN models, such as AlexNet [2], ResNet [3], and EfficientNet [4], have been proposed over the past decade and achieved unprecedented advances in a variety of vision problems, including image classification, object detection, semantic segmentation, and image processing to name a few. On the other hand, existing vision systems can be built on top of various input modalities as humans do, such as 2D images (*e.g.*, natural and medical images), videos, 3D data (*e.g.*, point clouds and meshes), as well as multimodal inputs (*e.g.*, image + text).

Despite the proliferation of CNN-based methods that excel at dealing with grid-like data structures like images, there is an emerging sense in the computer vision community that the non-grid topology information of data is crucial for representation learning but is yet to be thoroughly studied. Upon observing that human’s capacity for combinatorial

generalization largely relies on their cognitive mechanisms for representing structure and reasoning about relations [5], mimicking humans’ learning and decision-making processes could improve the vision model’s performance and provide logical pieces of evidence for the final prediction. For instance, in the task of object recognition, the state-of-the-art neural networks prefer to focus on perceiving the existence of objects separately, whereas the dependencies and interaction of different objects have received scant attention.

Moreover, compared to natural graph data, such as social networks and biological protein-protein networks, that has intrinsic edge connection and the notion of node, the construction of graph (*e.g.*, relation graph) based on regular grid data (*e.g.*, image and text) lacks principled approaches and critically depends on domain knowledge. On the other hand, some data formats in the vision problems, such as point clouds and meshes, are naturally not defined on a Cartesian grid and involve sophisticated relational information. In that sense, both regular and irregular visual data formats would benefit from the exploration of topological structures and relations especially on the challenging scenarios, such as understanding complex scene, learning from limited experience, and transferring knowledge across domains.

In the past few years, GNNs [6] have demonstrated ground-breaking performance in modeling graph structures under the umbrella of recent advancements of deep learning. In the scope of computer vision, much of current GNN-related research has one of the following two objectives: (1) a mixture of GNN and CNN backbones and (2) pure GNN architecture for representation learning. The former typically seeks to improve the long-range modeling ability

- C. Chen, H.-Y. Zhou, and Y. Yu are with the Department of Computer Science, The University of Hong Kong, Hong Kong. (email: cqchen1994@gmail.com, whuzhouhongyu@gmail.com, yizhouy@acm.org).
- Y. Wu, M. Xu, and X. Han are with the School of Science and Engineering, The Chinese University of Hong Kong, Shenzhen. Y. Wu and X. Han are also with the Future Network of Intelligence Institute, CUHK-Shenzhen. (email: 219019021@link.cuhk.edu.cn, mutianxu@link.cuhk.edu.cn, hanxiaoguang@cuhk.edu.cn).
- Q. Dai and S. Yang are with the School of Information Science and Technology, ShanghaiTech University, Shanghai. S. Yang is also with Shanghai Engineering Research Center of Intelligent Vision and Imaging. (email: daiqy2022@shanghaitech.edu.cn, yangsb@shanghaitech.edu.cn).

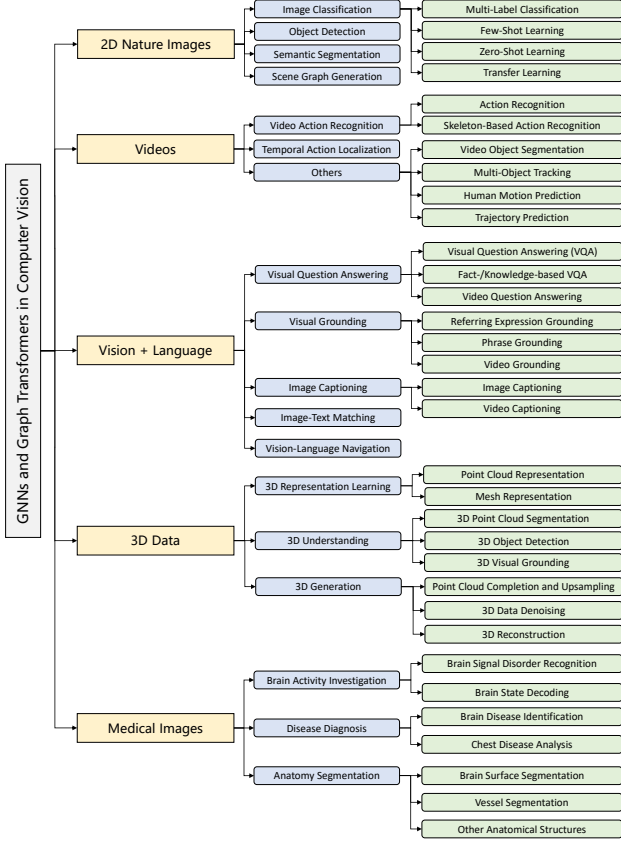


Fig. 1: The organization of this paper.

of CNN learned features and applies to vision tasks that are previously solved by pure CNN architectures, such as image classification and semantic segmentation. The latter serves as the feature extractor in some visual data formats, such as point clouds, and was developed in parallel compared to other directions. For instance, in the task of 3D shape classification on point clouds [7], there are three major research directions, namely, pointwise MLP methods, convolution-based methods, and graph-based methods.

Despite the fruitful achievements, however, there still does not exist a survey to systematically and timely review how GNN-based computer vision has progressed. Therefore, we write this literature review for the existing studies to provide a complete introduction of GNNs in computer vision from a task-oriented perspective, including (i) the definitions and challenges of the tasks, (ii) in-depth coverage of the representative approaches, and (iii) systematic discussions regarding insights, limitations, and future directions. Specifically, we categorize the applications of GNNs in computer vision into five types according to the modalities of input data. In each type, we categorize the applications according to the computer vision tasks they perform. We also review graph Transformers used in vision tasks considering their similarity with GNNs in terms of architecture [8], [9]. The organization of this survey is presented in Fig. 1.

## 2 BACKGROUND AND CATEGORIZATION

In this section, we recap GNNs and graph Transformers used in computer vision. Readers could refer to several previous GNN surveys [10], [11], [12] that comprehensively introduce the development of GNNs. In addition, we would like to

emphasize that many existing GNN-based vision approaches actually use a mixture of CNNs and GNNs, whereas we focus on the GNN side.

### 2.1 Recurrent GNNs

GNN was initially developed in the form of recurrent GNNs. Earlier work [6] in this regime tries to extract node representations from directed acyclic graphs by recurrently using the same set of weights over iterations. Scarselli *et al.* [13] extended such neural networks to process more types of graphs, such as cyclic and undirected graphs. They recurrently update the hidden state  $\mathbf{h}$  of a node as follows,

$$\mathbf{h}_i^{(t+1)} = \sum_{v_j \in \mathcal{N}(v_i)} f(\mathbf{x}_i, \mathbf{x}_j, \mathbf{x}_{ij}^e, \mathbf{h}_j^{(t)}), \quad (1)$$

where  $\mathcal{N}(v_i)$  represents the neighborhood of node  $v_i$ ,  $f(\cdot)$  is a feedforward neural network,  $\mathbf{x}_i \in \mathbb{R}^d$  denotes the features at  $v_i$ ,  $\mathbf{x}_{ij}^e \in \mathbb{R}^c$  denotes the features at the edge between  $v_i$  and  $v_j$ , and  $t$  is the iteration number.

### 2.2 Convolutional GNNs

Inspired by the astonishing progress of CNNs in the deep learning era, many research efforts have been devoted to generalizing convolution to the graph domain. Among them, there are two series of approaches (cf. Fig. 2) that garner the most attention in recent years, namely, the spectral approaches [14], [15], [16], [17], [18], [19] and the spatial approaches [20], [21], [22], [23], [24], [25].

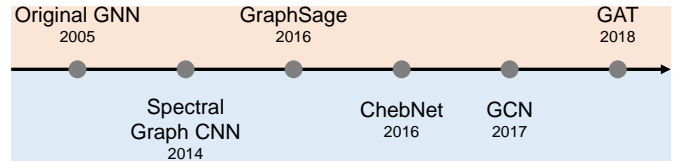


Fig. 2: Two types of graph convolutional operations.

#### 2.2.1 Spectral Approaches

Spectral approaches rely on the Laplacian spectrum to define graph convolution. For an undirected graph  $\mathcal{G} = \{\mathcal{V}, \mathcal{E}\}$ ,  $\mathbf{A}$  is the adjacency matrix, and  $\mathbf{D}$  is the diagonal degree matrix,  $\mathbf{D}_{ii} = \sum_j \mathbf{A}_{ij}$ .  $\mathbf{L} = \mathbf{I} - \mathbf{D}^{-1/2} \mathbf{A} \mathbf{D}^{-1/2}$  represents the normalized Laplacian matrix of  $\mathcal{G}$ , and  $\mathbf{L}$  can be decomposed as  $\mathbf{L} = \mathbf{U} \mathbf{\Lambda} \mathbf{U}^T$ , where  $\mathbf{U}$  is the matrix of eigenvectors and  $\mathbf{\Lambda} = \text{diag}[\lambda_1, \dots, \lambda_N]$  is the diagonal matrix of eigenvalues. Let  $\mathbf{Z} \in \mathbb{R}^{N \times d}$  ( $N = |\mathcal{V}|$ ) be the feature matrix of  $\mathcal{G}$ , and  $\mathbf{z} \in \mathbb{R}^N$  be one of the columns of  $\mathbf{Z}$  ( $d = 1$ ). The graph Fourier transform of  $\mathbf{z}$  is formulated as  $\mathcal{F}(\mathbf{z}) = \mathbf{U}^T \mathbf{z}$ , and the inverse graph Fourier transform is  $\mathcal{F}^{-1}(\hat{\mathbf{z}}) = \mathbf{U} \hat{\mathbf{z}}$ , where  $\hat{\mathbf{z}} = \mathcal{F}(\mathbf{z})$ . Then, the convolution of  $\mathbf{z}$  with a filter  $\mathbf{g} \in \mathbb{R}^N$  is defined as  $\mathbf{z} *_{\mathcal{G}} \mathbf{g} = \mathcal{F}^{-1}(\mathcal{F}(\mathbf{z}) \odot \mathcal{F}(\mathbf{g})) = \mathbf{U}((\mathbf{U}^T \mathbf{z}) \odot (\mathbf{U}^T \mathbf{g}))$ , where  $*$  is the graph convolution operator and  $\odot$  is the Hadamard product. By defining  $\mathbf{g}_{\theta} = \text{diag}(\mathbf{U}^T \mathbf{g})$ , which is a function of  $\mathbf{\Lambda}$ , we have

$$\mathbf{z} *_{\mathcal{G}} \mathbf{g} = \mathbf{U} \text{diag}(\mathbf{U}^T \mathbf{g}) \mathbf{U}^T \mathbf{z} = \mathbf{U} \mathbf{g}_{\theta} \mathbf{U}^T \mathbf{z}. \quad (2)$$

**Chebyshev Spectral CNN (ChebNet)** [16] uses Chebyshev polynomials to approximate the filtering operation  $\mathbf{g}_{\theta}$ .  $\mathbf{g}_{\theta} \approx \sum_{i=0}^K \theta_i T_k(\tilde{\mathbf{L}})$ , where  $\tilde{\mathbf{L}} = 2\mathbf{L}/\lambda_{max} - \mathbf{I}$  is the scaled

Laplacian matrix,  $\lambda_{max}$  is the largest eigenvalue of  $\mathbf{L}$ , and  $\theta_i$ 's are learnable parameters. The Chebyshev polynomials can be defined recursively by  $T_i(\mathbf{z}) = 2\mathbf{z}T_{i-1}(\mathbf{z}) - T_{i-2}(\mathbf{z})$  with  $T_0(\mathbf{z}) = 1$  and  $T_1(\mathbf{z}) = \mathbf{z}$ . Then, the filtering operation is formulated as

$$\mathbf{z} *_{\mathcal{G}} \mathbf{g} \approx \mathbf{U} \left( \sum_{i=0}^K \theta_i T_i(\tilde{\mathbf{L}}) \right) \mathbf{U}^T \mathbf{z} \approx \sum_{i=0}^K \theta_i T_i(\tilde{\mathbf{L}}) \mathbf{z}. \quad (3)$$

**Graph Convolutional Networks (GCNs)** [17] introduce a first-order approximation of ChebNet ( $K = 1$ ). A GCN iteratively aggregates information from neighbors, and the feed forward propagation regarding node  $v_i$  is conducted as

$$\mathbf{h}_i^{(l+1)} = \sigma \left( \sum_{v_j \in \mathcal{N}(v_i) \cup \{v_i\}} \hat{a}(v_i, v_j) \mathbf{W}^{(l)} \mathbf{h}_j^{(l)} \right), \quad (4)$$

where  $\sigma(\cdot)$  is a nonlinear activation function,  $\hat{\mathbf{A}} = (\hat{a}(v_i, u_j))$  denotes the re-normalized adjacency matrix  $\mathbf{A}$ , and  $\mathbf{W}^{(l)}$  is a learnable transformation matrix in the  $l$ -th layer. GCNs can also be interpreted from a spatial view [12].

### 2.2.2 Spatial Approaches

**GraphSAGE** [22] is a general inductive framework that updates node states by sampling and aggregating hidden states from a fixed number of local neighbors. Formally, it performs graph convolutions in the spatial domain,

$$\begin{aligned} \mathbf{h}_{\mathcal{N}_s(v_i)}^{(l+1)} &= \text{Aggregator}_{l+1} \left( \{ \mathbf{h}_j^l, \forall v_j \in \mathcal{N}_s(v_i) \} \right), \\ \mathbf{h}_i^{(l+1)} &= \sigma \left( \mathbf{W}^{(l+1)} \cdot [\mathbf{h}_{v_i}^l \oplus \mathbf{h}_{\mathcal{N}_s(v_i)}^{(l+1)}] \right), \end{aligned} \quad (5)$$

where  $\mathcal{N}_s(v_i)$  is a subset of nodes sampled from the full neighborhood  $\mathcal{N}(v_i)$ , and  $\oplus$  is the concatenation operator. As suggested by [22], the aggregation function  $\text{Aggregator}_l$  can be the mean aggregator, LSTM aggregator, or pooling aggregator.

**Graph Attention Networks (GAT)** [23] introduces a self-attention mechanism to learn dynamic weights between connected nodes. It updates the hidden state of a node by attending to its neighbors,

$$\begin{aligned} \mathbf{h}_i^{(l+1)} &= \sigma \left( \sum_{v_j \in \mathcal{N}(v_i) \cup \{v_i\}} \alpha_{ij} \mathbf{W}^{(l)} \mathbf{h}_j^{(l)} \right), \\ \alpha_{ij} &= \frac{\exp \left( \text{LReLU}(\mathbf{a}_{(l)}^T [\mathbf{W}^{(l)} \mathbf{h}_i^{(l)} \oplus \mathbf{W}^{(l)} \mathbf{h}_j^{(l)}]) \right)}{\sum_{v_k \in \mathcal{N}(v_i)} \exp \left( \text{LReLU}(\mathbf{a}_{(l)}^T [\mathbf{W}^{(l)} \mathbf{h}_i^{(l)} \oplus \mathbf{W}^{(l)} \mathbf{h}_k^{(l)}]) \right)} \end{aligned} \quad (6)$$

where  $\alpha_{ij}$  is the pairwise attention weight and  $\mathbf{a}$  is a vector of learnable parameters. To increase the model's capacity and make the process of self-attention stable, GAT employs multi-head self-attention in practice.

### 2.2.3 New GNN Techniques

**Deeper GNNs.** A few recent works [26], [27], [28] delve into building deep GCNs for a variety of basic graph-oriented tasks, such as node prediction and link prediction. DeepGCNs [27] introduce commonly used concepts in CNNs—residual connections, dense connections, and dilated convolutions—to make GCNs go deeper as CNNs. By doing so, they could implement a 56-layer GCN for point cloud semantic segmentation. Rong *et al.* [28] propose the DropEdge training strategy to alleviate the over-fitting

and over-smoothing problems of deep GCNs. Technically, DropEdge randomly drops out certain proportion of edges of the input graph for each training iteration. Moreover, Li *et al.* [29] systemically investigate the effects of reversible connections, group convolutions, weight tying, and equilibrium models for improving the memory and parameter efficiency of GNNs, empirically revealing that combining reversible connections with deep network architectures could enable the training of extremely deep and wide GNNs (1001 layers with 80 channels each and 448 layers with 224 channels each).

**Graph Pooling.** Graph pooling is a critical operation for modern GNN architectures. Inspired by the traditional CNN-based pooling, most approaches formulate graph pooling as a cluster assignment problem, extending the idea of local patches in regular grids to graphs. Defferrard *et al.* [16] achieve graph Pooling with pre-defined subgraphs produced by a graphcut algorithm. Ying *et al.* [30] propose a differentiable graph pooling module, named DIFFPOOL, that can generate hierarchical representations of graphs and can be combined with various GNN architectures in an end-to-end fashion. Mao *et al.* [31] introduce EigenPooling, which incorporates node features and local structures to obtain better assignment matrices. Gao *et al.* [32] present a U-shaped architecture, termed Graph U-Nets, to implement pooling and up-sampling operations for GNNs.

**Vision GNN.** Very recently, Han *et al.* [33] propose a Vision GNN (ViG) architecture to represent an image as a graph, aiming to learn graph-level features for downstream vision tasks. ViG first splits the input image into a set of regularly-shaped patches and regards each patch as a graph node. Next, graph edges are constructed using K-nearest neighbors of each node. Then, multi-head graph convolution and positional encoding are performed at every node to jointly learn the topological structure and node features, and a feed-forward network (FFN) is used to mitigate the over-smoothing of node features and enhance the feature transformation capacity. The proposed ViG achieves competitive results on recognition and detection benchmarks. For example, ViG outperforms DeiT by 1.7% (top-1 accuracy) on ImageNet classification and Swin-T by 0.3% (mAP) on MSCOCO object detection.

## 2.3 Graph Transformers for 3D Data

**Point Transformer** [34] designs a local vector self-attention mechanism for point cloud analysis. In contrast, a related work, Point Cloud Transformer [35], adopts global attention. The local vector self-attention operation in each Transformer block of the Point Transformer is defined as,

$$\begin{aligned} \mathbf{h}_i^{(l+1)} &= \\ &\sum_{v_j \in \mathcal{N}_s(v_i)} \rho \left( \gamma \left( \mathbf{W}_Q^{(l+1)} \mathbf{h}_i^{(l)} - \mathbf{W}_K^{(l+1)} \mathbf{h}_j^{(l)} + \delta \right) \right) \odot \left( \mathbf{W}_V^{(l+1)} \mathbf{h}_j^{(l)} + \delta \right), \end{aligned} \quad (7)$$

where  $\mathbf{W}_Q$ ,  $\mathbf{W}_K$ ,  $\mathbf{W}_V$  are shared parameter matrices to compute the query, key and value for attention-based aggregation,  $\odot$  is the element-wise product,  $\delta$  is a position encoding function,  $\gamma$  is a nonlinear mapping function (e.g. MLP), and  $\rho$  is a normalization function (e.g. softmax). Recently, Fast Point Transformer [36] introduces a lightweight local self-attention architecture with voxel hashing to significantly improve efficiency. Stratified Transformer [37] samples distant points

as additional keys to enlarge the receptive field, thereby modeling long-range dependencies.

**Mesh Graphormer** [38] develops a graph Transformer for mesh reconstruction from images. It exploits graph convolution and self-attention to learn local interactions within neighborhoods and non-local relations, respectively. Each Graphormer encoder block consists of five components, *i.e.*, a Layer Norm, a Multi-Head Self-Attention (MHSA) module, a Graph Residual Block, a second Layer Norm, and an MLP at the end. Specifically, the MHSA module with  $P$  heads accepts an input sequence  $\mathbf{H} = \{\mathbf{h}_i\} \in \mathbb{R}^{n \times d}$ ,  $i \in \{1, 2, \dots, n\}$  of  $n$  tokens, and outputs  $\{\mathbf{h}_i^p\}$  for each token, where  $p \in \{1, 2, \dots, P\}$  is the head index. Each  $\mathbf{h}_i^p$  is computed as

$$\mathbf{h}_i^p = \text{Att}(\mathbf{Q}_i^p, \mathbf{K}^p) \cdot \mathbf{V}^p \in \mathbb{R}^{\frac{d}{P}}, \quad (8)$$

where  $\mathbf{Q}, \mathbf{K}, \mathbf{V}$  are computed as  $\mathbf{H}\mathbf{W}_Q, \mathbf{H}\mathbf{W}_K, \mathbf{H}\mathbf{W}_V$ , respectively,  $\mathbf{W}_Q, \mathbf{W}_K, \mathbf{W}_V$  are trainable parameter matrices in each layer,  $\text{Att}(\cdot)$  computes the original self-attention in [39], and  $\mathbf{Q}_i^p \in \mathbb{R}^{\frac{d}{P}}, \mathbf{K}^p, \mathbf{V}^p \in \mathbb{R}^{n \times \frac{d}{P}}$ . Graph convolution (*i.e.* Eq. 4) with a residual connection is further applied to  $\mathbf{H}$ .

### 3 2D NATURAL IMAGES

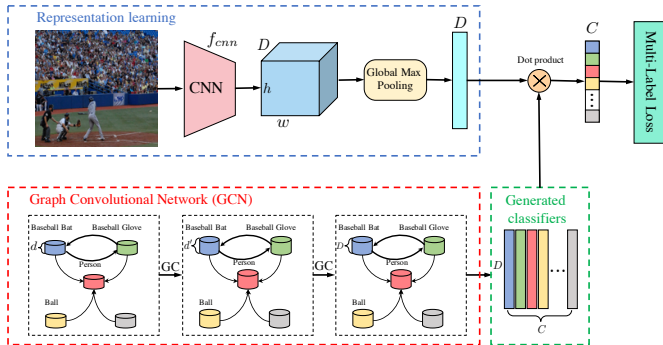


Fig. 3: ML-GCN (Figure used courtesy of [40]).

#### 3.1 Image Classification

##### 3.1.1 Multi-Label Classification

Compared to traditional methods that treat the objects in isolation, ML-GCN [40] (*cf.* Fig. 3) builds a directed graph on the basis of label space, where each node stands for an object label (word embeddings) and their connections model the inter-dependencies of different labels. Multiple GCN layers are then applied to project label representations into a set of inter-dependent classifiers and a label correlation matrix is introduced to induce the information propagation among nodes. Instead of learning semantic representations and label-dependencies in parallel, Chen *et al.* [41] introduce the statistical label co-occurrence to directly guide graph propagation among semantic features of different object regions. Several follow-up methods [42], [43], [44] strive to model the label dependencies via more elaborate GNN architectures, such as hypergraph neural networks [43], and attention-driven GCN [44]. You *et al.* [45] propose a cross-modality attention mechanism to aggregate visual features and label embeddings for generating category-wise attention maps. In particular, Nguyen *et al.* [46] first decompose the label graph into multiple sub-graphs and then introduce

TABLE 1: Performance (mAP) on two multi-label classification benchmarks, *i.e.*, MS-COCO and VOC 2007.

Method	Reference	MS-COCO	VOC 2007
ResNet-101 [3]	CVPR'16	77.3	89.9
ML-GCN [40]	CVPR'19	83.0	94.0
SSGRL [41]	ICCV'19	83.8	93.4
MS-CMA [45]	AAAI'20	83.8	-
ADD-GCN [44]	ECCV'20	85.2	93.6
TDRG [47]	ICCV'21	86.0	95.0

graph Transformers to exploit the semantic and topological relations among object labels. Recently, Zhao *et al.* [47] introduce GCN to model the class-wise dependencies under the guidance of structural relations learned by Transformer units. As shown in Tab. 1, we summarize the performance of some of the discussed methods on standard benchmarks.

##### 3.1.2 Few-Shot Learning (FSL)

Garcia *et al.* [48] formulate FSL as a supervised interpolation problem on a densely-connected graph, where the vertices stand for images in the collection and the adjacency is learnable with trainable similarity kernels. They also extend the proposed method to semi-supervised and active learning tasks. TPN [49] constructs graphs on the top of embedding space to fully exploit the manifold structure of the novel classes. Label information is propagated from the support set to the query set based on the constructed graphs. Compared to the above node-labeling framework, Kim *et al.* [50] propose an edge-labeling GNN framework that learns to predict edge labels, explicitly constraining the intra- and inter-class similarities. Luo *et al.* [51] formulate meta-learning-based FSL as continual learning of a sequence of tasks and resort to Bayesian GNN to capture the intra- and inter-task correlations. Yang *et al.* [52] devise a dual complete graph network to model both distribution- and instance-level relations. Chen *et al.* [53] exploit the hierarchical relationships among graph nodes via the bottom-up and top-down reasoning modules. Instead of using GNN to perform label propagation, Yu *et al.* [54] introduce an instance GNN and a prototype GNN as feature embedding task adaptation modules for quickly adapting learned features to new tasks.

##### 3.1.3 Zero-Shot Learning (ZSL)

GNN-based ZSL methods have attracted increasing attention for representing and propagating common knowledge between seen and unseen classes. To improve the knowledge propagation between distant nodes in a shallow GCN, Kampffmeyer *et al.* [55] propose a Dense Graph Propagation (DGP) module to exploit the hierarchical structure of knowledge graph. DGP consists of two phases to iteratively propagate knowledge between a node and its ancestors and descendants. Xie *et al.* [56] represent each input image as a region graph, where each node stands for an attended region in the image and the edges are appearance similarities among these region nodes. Then, a GCN is applied to capture the appearance relationships among these local regions. Instead of pre-defined attribute space in the context ZSL, APNet [57] generates and updates attribute vectors with an attribute propagation network for optimizing the attribute space. Liu *et al.* [58] introduce the visual and semantic prototype propagation on auto-generated graphs to enhance

the inter-class relations and align the corresponding class-wise dependencies in visual and semantic space. Mancini *et al.* [59] investigate the problem of open world compositional ZSL (OW-CZSL) by introducing a Compositional Cosine Graph Embedding (Co-CGE) model to learn the relationship between primitives and compositions through a GCN. They quantitatively measure the feasibility scores of a state-object composition and incorporate the computed scores into Co-CGE in two ways (as margins for a cross-entropy loss and as weights for the graph edges). Chen *et al.* [60] resort to GAT for exploiting the appearance relations between local regions and the cooperation between local and global features.

### 3.1.4 Transfer Learning

Domain Adaptation (DA) and Domain Generalization (DG), which are two subtopics of transfer learning, resort to knowledge graphs for representing the relationships among different classes. Such knowledge graphs are expected to be transferable across domains and can be reused for novel environments. Wang *et al.* [61] propose a Graph Convolutional Adversarial Network (GCAN) for DA, where a GCN is developed on top of densely-connected instance graphs to encode data structure information. Here, the graphs are constructed on mini-batch samples and thus could be end-to-end trainable. For multi-target DA, Yang *et al.* [62] build a heterogeneous relation graph and introduce GAT to propagate the semantic information and generate reliable pseudo-labels. Roy *et al.* [63] introduce a GCN to aggregate information from different domains along with a co-teaching and curriculum learning strategy to achieve progressive adaptation. Luo *et al.* [64] study the problem of open-set DA via a progressive graph learning framework to select pseudo-labels and thus avoid the negative transfer. Wang *et al.* [65] gradually attain cross-domain prototype alignment based on features learned from different stages of GNNs. Wang *et al.* [66] introduce a knowledge graph based on the prototypes of different domains to perform information propagation among semantically adjacent representations. Chen *et al.* [67] build global prototypical relation graphs and introduce a graph self-attention mechanism to model the long-range dependencies among different categories. They update the constructed global relation graphs using mini-batch samples in a moving average manner.

**Discussion.** GNNs used for image classification have been mostly explored for multi-object, data- or label-efficient scenarios (*e.g.*, zero-shot and few-shot learning), aiming to model the complex relations among different objects/classes for compensating the shortage of training samples or supervision signals. Current work focuses on extracting ad-hoc knowledge graphs from the data for a certain task, which is heuristic and relies on the human prior. Future work is expected to (i) develop general and automatic graph construction procedures, (ii) enhance the interactions between abstract graph structures and task-specific classifiers, and (iii) excavate more fine-grained building blocks (node and edge) to increase the capability of constructed graphs.

## 3.2 Object Detection

Object detection [68] aims to localize and recognize all object instances of given classes in digital images. From

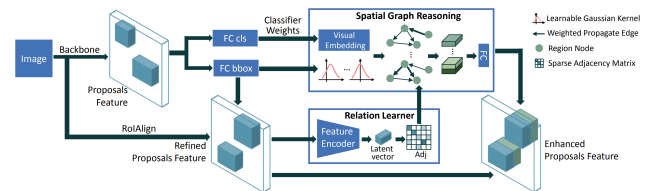


Fig. 4: SGRN (Figure used courtesy of [71]).

the architecture point of view, existing objection detection frameworks can be categorized into two types: two-stage and one-stage object detectors. Despite their fruitful progress, modern object detectors often neglect the relations and interactions of object instances by processing a set of objects individually [69]. As a consequence, existing methods may still be confined by two challenges. First, when data distributions embody structural object relations, how to embed the object-level dependencies into the detection pipeline is yet to be thoroughly studied. Second, prevailing approaches excel at perceiving the existence of objects by mapping the representations of objects into a common latent space, while lacking the ability of reasoning over semantic dependencies, co-occurrence, and relative locations of objects.

Reasoning-RCNN [70] presents an adaptive global reasoning network for large-scale object detection by incorporating commonsense knowledge (category-wise knowledge graph) and propagating visual information globally, thereby endowing detection networks with the capability of reasoning. SGRN [71] goes one step further by adaptively discovering semantic and spatial relationships without requiring prior handcrafted linguistic knowledge. As shown in Fig. 4, the relation learner learns a sparse adjacency matrix to encode the contextual relations among different regions. Then, a spatial graph reasoning module is introduced to perform feature aggregation and relational reasoning with the help of a learned adjacency matrix and learnable spatial Gaussian kernels. RelationNet [69] introduces an adapted attention module to detection head networks, explicitly learning information between objects through encoding the long-range dependencies. RelationNet++ [72] presents a self-attention-based decoder module to embrace the strengths of different object/part representations within a single detection framework. Li *et al.* [73] introduce a heterogeneous graph to jointly model object-object and object-scene relations. Zhao *et al.* [74] propose a graph feature pyramid network (GraphFPN), which explores the contextual and hierarchical structures of an input image based on a superpixel hierarchy, enabling within-scale and cross-scale feature interactions with the help of spatial and channel attention mechanisms. This work can be used as a plug-and-play component in a series of detectors, such as RetinaNet and Faster R-CNN.

In addition to improving the in-distribution performance, how to generalize object detection models to novel environments (*e.g.*, new domains or categories) has attracted a great deal of attention in many real-world applications. In particular, domain adaptive object detection (DAOD) is one of the most promising problems. FGRR [75], [76] first builds intra- and inter-domain relation graphs in virtue of cyclic between-domain consistency without any prior knowledge about the target distribution. Then, it introduces the graph attention mechanisms and bipartite GCNs to model

the homogeneous and heterogeneous object dependencies and interactions on both pixel and semantic spaces. In addition, SIGMA [77] formulates DAOD as a graph matching problem by establishing cross-image graphs to model class-conditional distributions on both domains. SRR-FSD [78] introduces a semantic relation reasoning module to integrate semantic information between base and novel classes for novel object detection, where each class is instantiated as a node of the dynamic relation graph. By doing so, the semantic information is propagated through nodes methodically, endowing the detector with semantic reasoning ability.

**Discussion.** Owing to the long-range modeling capability, GNN-based detection methods exploit between-object [71], cross-scale [74] or cross-domain [75] relationships, as well as relationships between base and novel classes [78]. Due to the introduction of additional learning modules, however, the optimization process becomes harder than vanilla detection models. Moreover, the compatibility between Euclidean and non-Euclidean structures will be challenged if not properly harmonized. In future, researchers could (i) design better region-to-node feature mapping methods, (ii) incorporate Transformer (or pure GNN) encoders to improve the expressive power of initial node features, and (iii) instead of resorting to forward and backward feature mappings, directly perform reasoning in the original feature space to better preserve the intrinsic structure of images.

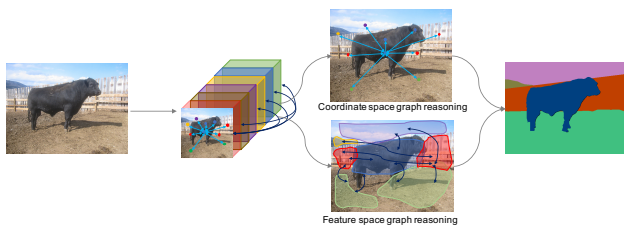


Fig. 5: DGCNet (Figure used courtesy of [79]).

### 3.3 Image Segmentation

Semantic segmentation aims to divide a given image into several semantically meaningful regions by conducting pixel-wise labeling, which provides rich information regarding object appearances and contexts. Albeit CNN-based architectures have revolutionized the segmentation tasks, the intrinsic limitations of convolutional operations (*e.g.*, cannot reason among distant regions of arbitrary shape) inevitably compromise their further improvements and pose great challenge for obtaining holistic understanding of the scenes.

DGCNet [79] targets on modeling the global context of input features via a dual GCN framework (cf. Fig. 5), where a coordinate space GCN models spatial relationships between pixels in the image, and a feature space GCN models dependencies along the channel dimensions of the network’s feature map. After reasoning, these two complementary relation-aware feature are mapped back to the original coordinate space and added to the original feature. Chen *et al.* [80] design the global reasoning unit by projecting features that are globally aggregated in coordinate space to node domain and performing relational reasoning in a fully-connected graph. To model long-range dependencies and avoid the construction of fully-connected graphs, DGMN [81] dynamically samples the neighborhood of a node and then

TABLE 2: Performance (mIOU) on segmentation benchmarks, *i.e.*, Cityscapes, PASCAL-Context, and COCO Stuff.

Method	Reference	Cityscapes	PASCAL	COCO Stuff
DGCNet [79]	BMVC’19	80.5	53.7	-
GloRe [80]	CVPR’19	80.9	-	-
DGMN [81]	CVPR’20	81.6	-	-
SpyGR [83]	CVPR’20	81.6	52.8	39.9
RGNet [82]	ECCV’20	81.5	53.9	-
CDGCNet [84]	ECCV’20	82.0	-	40.7

predicts the node dependencies, filter weights, and affinity matrix to attain information propagation. Concurrently, Yu *et al.* [82] propose to dynamically sample some representative nodes for relational modeling. Instead of constructing additional semantic interaction spaces (projecting and re-projecting), Li *et al.* [83] propose an improved Laplacian formulation that enables graph reasoning in the original feature space, fully exploiting the contextual relations at different feature scales. Hu *et al.* [84] introduce a class-wise dynamic graph convolution module to conduct graph reasoning over the pixels that belong to the same class. The coarse segmentation results are used as the class-wise mask for graph construction and then class-wise graph reasoning is performed to dynamically aggregate features. As shown in Tab. 2, we summarize the performance of some of the discussed methods on standard benchmarks.

For one-shot semantic segmentation, Zhang *et al.* [85] introduce a pyramid graph attention module to model the connection between query and support feature maps, endowing unlabeled pixels in the query set with semantic and contextual information. For few-shot semantic segmentation, Xie *et al.* [86] propose a scale-aware GNN to perform cross-scale relational reasoning among support-query images. A self-node collaboration mechanism is introduced to perceive different resolutions of the same object. Zhang *et al.* [87] study the problem of weakly supervised semantic segmentation via affinity attention GNN. Specifically, an image will first be converted to a weighted graph via an affinity CNN network, and then an affinity attention layer is devised to obtain long-range interactions from the constructed graph and propagate semantic information to the unlabeled pixels. In addition to semantic segmentation, Wu *et al.* [88] design a bidirectional graph reasoning network to bridge the things branch and the stuff branch for panoptic segmentation. They first build things and stuff graphs to represent the intra-branch relations. Then, bidirectional graph reasoning is performed to propagate the semantic representations in both intra- and inter-branch.

**Discussion.** Many research efforts in semantic segmentation are devoted to exploring contextual information in the local- or global-level with pyramid pooling, dilated convolutions, or the self-attention mechanism. For instance, non-local networks [89] and their variants achieve this goal by adopting the self-attention mechanism, but are computationally expensive as comparing every pixel to all other pixels in an image has a quadratic time complexity. In addition, probabilistic graphical models, such as Conditional Random Fields (CRFs) and Markov Random Fields (MRFs), can be used to model scene-level semantic contexts but have very limited representation ability. In comparison to these prior efforts, GNN-based methods show clear superiority in terms of relation modeling and training efficiency.

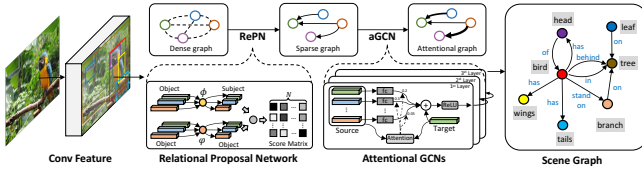


Fig. 6: Graph R-CNN (Figure used courtesy of [90]).

### 3.4 Scene Graph Generation (SGG)

SGG [91], [92] refers to the task of detecting object pairs and their relationships in an image to generate a visually-grounded scene graph, which provides a high-level understanding of the visual scene rather than treating individual objects in isolation. Technically, a scene graph parses the image by representing the objects as the nodes and their relations as the edges, perfectly fitting the nature of GNNs in comparison to other computer vision tasks that usually require prior knowledge to obtain abstract task-specific graph structures from inputs.

Current GNN-based SGG methods typically consist of three stages, namely, object detection, relation graph construction and refinement, and relation prediction. Here, we focus on the GNN-related modules, *i.e.*, relation graph construction and learning. Factorizable Net [93], which is a subgraph-based approach (*i.e.*, each subgraph is regarded as a node), has a spatially weighted message passing structure to refine the features of objects and subgroups by passing messages among them with attention-like schemes. Graph R-CNN [90] (cf. Fig. 6) first obtain a sparse candidate graph by pruning the densely-connected graph generated from RPN via a relation proposal network, then an attentional GCN is introduced to aggregate contextual information and update node features and edge relationships. Qi *et al.* [94] propose attentive relational networks, which first transform label word embeddings and visual features into a shared semantic space, and then rely on GAT to perform feature aggregation for final relation inference. Li *et al.* [95] introduce bipartite GNN to estimate and propagate relation confidence in a multi-stage manner. Suhail *et al.* [96] propose an energy-based framework, which depends on graph message passing algorithm for computing the energy of configurations.

## 4 VIDEO UNDERSTANDING

Some research has explored utilizing the GNNs in the field of video understanding, such as video action recognition [97], [98], temporal action localization [99], [100], and video object segmentation [101], [102]. As spatio-temporal relational reasoning is critical in video processing, these works usually applied GNNs to reason about the spatial and semantic relations between visual constituents over time.

### 4.1 Video Action Recognition

Video human action recognition is one of the fundamental tasks in video processing and understanding, which aims to identify and classify human actions in RGB/depth videos or skeleton data. Regardless of which modality is based, modeling the spatio-temporal context among joints, humans and objects is critical in identifying human action.

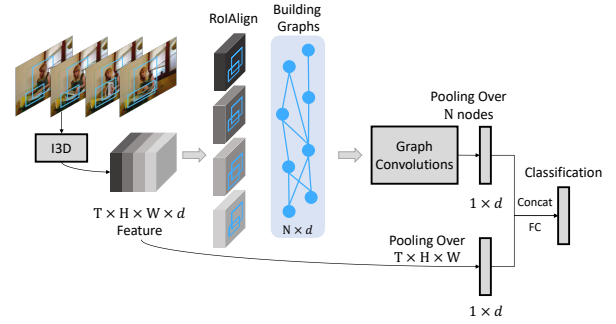


Fig. 7: Long-range temporal modeling via GCNs (Figure used courtesy of [97]).

**Action Recognition.** Wang *et al.* [97] propose to capture the long-range temporal contexts via graph-based reasoning over human-object and object-object relationships. As shown in Fig. 7, they connect all the humans and objects in all the frames to construct a space-time region graph where appearance-similarity edges and spatial-temporal edges connect between any two objects and spatially overlapping objects on consecutive frames, respectively. The results of the GCNs applied on the graph are used to predict human action. Ou *et al.* [103] improve the spatial-temporal graph in [97] by constructing actor-centric object-level graph and applying GCNs to capture the contexts among objects in a actor-centric way. In addition, a relation-level graph is built to inference the contexts in relation nodes. Instead of spatio-temporal modeling, Zhang *et al.* [104] propose multi-scale reasoning in the temporal graph of a video, in which each node is a frame in the video, and the pairwise relations between nodes are represented as a learnable adjacent matrix. In order to capture both short-term and long-term dependencies, GAT and the temporal adjacent matrix are designed as multi-head, where each head investigates one kind of temporal relation. Gao *et al.* [105] extend the GCN-based relation modeling to zero-shot action recognition. They leverage knowledge graphs to model the relations among actions and attributes jointly. Zhou *et al.* [106] introduce a graph-based high-order relation modeling method for long-term action recognition. They utilize a graph network to aggregate information from multiple graphs with different basic relations among objects, motions, and sub-actions to capture higher-order relations. In addition to human action recognition, GNNs have been used for group activity recognition [107] and action performance assessment [108]. Both methods apply multiple GCNs to reason different types of relations on the constructed graphs and aggregate the results from the GCNs for prediction.

**Skeleton-Based Action Recognition.** Skeleton data plays a vital role in action recognition because spatio-temporal dependencies among human body parts indicate human motion and action. Skeleton-based action recognition takes a video’s skeleton sequence as input and recognizes human actions. Considering the human skeleton is a graph structure with a natural joint connection, Yan *et al.* [98] propose a ST-GCN network first connects joints in a frame according to the natural connectivity in the human body and then connects the same joints in two consecutive frames to maintain temporal information. They perform GCNs on the joint graph to learn both spatial and temporal patterns of actions. As shown in Tab. 3, GNN-based ST-GCN network improves

Method	Charades [116] mAP	NTU-RGB+D [117] Accuracy(%)		Kinetics Skeleton [118] Accuracy(%)	
		X-Sub	X-View	Top1	Top5
Action Recognition					
NL + I3D [89]	37.5	-	-	-	-
STRG [97]*	39.7	-	-	-	-
$OR^2G$ [103]*	44.9	-	-	-	-
TS-GCN [105]*	40.2	-	-	-	-
GHRM [106]*	38.3	-	-	-	-
Skeleton-Based Action Recognition					
Deep LSTM [117]	-	60.7	67.3	16.4	35.3
ST-GCN [98]*	-	81.5	88.3	30.7	52.8
2s-AGCN [109]*	-	88.5	95.1	36.1	58.7
STGR [110]*	-	86.9	92.3	33.6	56.1
AS-GCN [111]*	-	86.8	94.2	34.8	56.5
Zhao et al. [112]*	-	81.8	89.0	-	-
DGNN [114]*	-	89.9	96.1	36.9	59.6
MS-G3D Net [115]*	-	91.5	96.2	38.0	60.9

TABLE 3: Performance comparison on datasets for action recognition. GNN-based methods are marked with \*.

previous methods significantly. Shi *et al.* [109] improve [98] by introducing a fully-connected graph with learnable edge weights between joints and a data-dependent graph learned from the input skeleton. They build GCNs on the three graphs. Similar to [109], Li *et al.* [110] and Li *et al.* [111] also connect physically-apart skeleton joints to captures the patterns of collaborative moving joints. Different from [110], Zhao *et al.* [112] improves the joints’ connection in a single frame [98] by adding edges between limbs and head. In addition, they use GCNs to capture joints’ relations in single frames and adopt the LSTM [113] to capture the temporal dynamics. Instead of only updating node features in GCNs, Shi *et al.* [114] introduce to maintain edge features and learn both node and edge feature representations via directed graph convolution. Unlike previous works that model local spatial and temporal contexts in consecutive frames, Liu *et al.* [115] capture long-range spatial-temporal dependencies. Specifically, they first construct multiple dilated windows over temporal dimension. Then, in each window, they separately utilize GCNs on multiple graphs with different scales. Finally, they aggregate the results of GCNs on all the graphs in multiple windows to capture multi-scale and long-range dependencies.

Some works have explored modifying standard graph convolution layers to better adapt to action recognition. Si *et al.* [119] incorporate GCNs into LSTM units by obtaining GCN-based updates of gates, hidden state, and cell memory. Inspired by shift CNNs [120], Cheng *et al.* [121] propose shift graph convolution networks by having multiple feature partitions at a joint and updating each of them using the features at its corresponding neighboring joint. Cheng *et al.* [122] propose to decouple aggregation in GCNs by splitting channels into multiple groups and learning the adjacency matrix for each group independently.

## 4.2 Temporal Action Localization

Temporal action localization aims to localize temporal intervals and recognize action instances from an untrimmed video. Video context plays important role for action detection as it can be used to infer potential actions [100]. This section reviews methods that utilize GNNs to obtain video context.

Zeng *et al.* [99] follow a two-stage pipeline for temporal action localization, which first generates temporal proposals and then classify and regress temporal boundary for

proposals. In the second stage, any pairwise proposals are connected based on their temporal intersection over union and the  $L_1$  distance over union to form a proposal graph. GCNs are performed on the graph to capture the relations among proposal, and the output of GCNs is used to predict the boundary and category for each proposal. Unlike [99] takes temporal proposals as nodes, Xu *et al.* [100] propose to present video sequence as a snippet graph where each node is a snippet, and each edge corresponds to the correlation between snippets. Both temporal edges between snippets in two consecutive time steps and semantic edges learned from snippets features are considered in the graph connectivity. A dynamic graph convolution operation [123] is used to obtain temporal and semantic context of snippets. Zhao *et al.* [124] introduce a video self-stitching graph network to address the scaling curse in [100] by utilizing graph network to exploit multi-level correlations among cross-scale snippets. Besides temporal action localization, [125] and [126] utilize GNNs in temporal action proposal generation and video action segmentation, respectively.

## 4.3 Others

**Video Object Segmentation** Wang *et al.* [101] adopt GNNs to capture the high-order relations among video frames to help segment objects from a global perspective. In addition, they extend the convolution operations in classical GNNs to adapt to the pixel-level segmentation task. Lu *et al.* [102] extends [101] by introducing a graph memory network to store memory in a graph structure with memory cells as nodes. And the query between the current frame and the memory graph help to predict the segmentation mask of the current frame.

**Multi-Object Tracking** aims to track all the object instances in a video. Two-step tracking-by-detection methods take object detections of all frames as nodes and the connection between pairwise objects in different frames as edges. Grouping nodes into connected components can obtain the trajectories of objects. Braso *et al.* [127] propose a time-aware message passing network on the detection graph to encode the temporal structure of the graph and predict whether edges are active or non-active to obtain the connected components. Weng *et al.* [128] suggest first connecting tracked objects and detected objects in two consecutive frames based on their spatial distances. Then, the GNNs [123] are used to aggregate features of neighbors to the current nodes and regress the edges to obtain the connectivity between the tracked objects and the detected ones.

**Human motion prediction** is the task of forecasting future poses given the past motions in videos. Like the skeleton-based action recognition, the spatio-temporal correlation among body parts is a crucial cue for accurate motion prediction. Li *et al.* [129] propose dynamic multi-scale GNNs to capture physical constraints and movement relations among body components at multiple scales and achieves effective motion prediction. Instead of modeling spatial correlation, Sofianos *et al.* [130] allow encoding both spatial joint-joint, temporal time-time, and spatio-temporal joint-time interactions via the proposed separable space-time GNNs. In addition to human motion prediction, Cai *et al.* [131] utilize the GNNs to estimate the 3D human pose from the consecutive 2D poses.



**Trajectory Prediction** aims to predict the future pedestrian trajectory by relying on the historical trajectory and the complex interactions between the pedestrian and the environment/other pedestrians. Mohamed *et al.* [132] propose constructing a graph representation of pedestrian trajectory based on relative locations among pedestrians and their temporal information. Furthermore, the GCNs are applied to capture the complex interactions and the graph’s spatio-temporal representation. Similar to [132], Yu *et al.* [133] propose a spatio-temporal graph Transformer to conduct crowd trajectory prediction based on the pedestrians’ relative locations and temporal trajectory dependencies. In addition, they extend GATs by using Transformer’s attention mechanism [39]. Beyond the relative distance of pedestrians, Sun *et al.* [134] utilize the social related annotations, historical trajectory, and human context to construct the social behavior graph with pedestrians’ historical trajectories as nodes and the relational social representation as edges. Then, they apply GCNs on the graph to learn high-order social relations to facilitate the future trajectory generation. Shi *et al.* [135] use the same GCNs in [132] to capture the spatial and temporal dependencies but they introduce two sparse directed spatial and temporal graph representations for trajectories. Different from previous methods, Li *et al.* [136] construct a multi-scale graph to model the spatial information and surrounding area of pedestrians in multiple scales. In addition, they use scene semantic segmentation to help model the relations between pedestrians and the scene.

#### 4.4 Discussion

Compared to images, videos involve temporal connectivity patterns among consecutive frames. The spatio-temporal dependencies and contexts in a video play an essential role in video understanding. Therefore, since the introduction of GNNs for capturing the spatial and semantic relations among visual constituents over time, video understanding has achieved significant progress. However, existing methods usually either capture partial dependencies at the frame level or local contexts at the region level for several consecutive frames. A meaningful direction for future research would be effectively capturing long-range global dependencies or crucial contexts without redundant information.

## 5 VISION + LANGUAGE

In addition to single modality, there has been growing interest in applying GNNs to vision-and-language tasks, such as visual question answering [137], visual grounding [138], and image captioning [139]. GNNs facilitate modeling the structure of visual and linguistic components to help with cross-modal semantic alignment and joint understanding.

### 5.1 Visual Question Answering

In visual question answering (VQA), a question is provided as text in natural language together with an image, and a correct answer requires to be predicted. Since questions usually describe not only the appearances and attributes but also the relations between the images’ visual constituents, capturing the relations and aligning them with the questions plays a vital role for VQA.

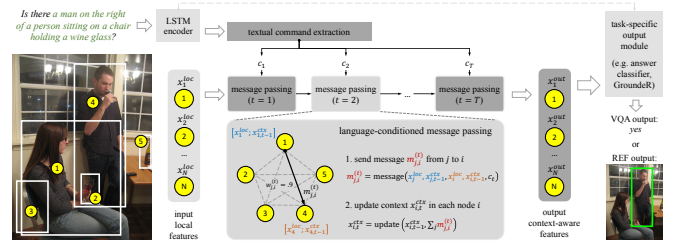


Fig. 8: Language-Conditioned Graph Networks (Figure used courtesy of [144]).

**Visual Question Answering.** Teney *et al.* [140] first introduce the graph representations of images and questions and then align the constructed graphs for VQA. Specifically, the image graph is with objects as nodes and relative spatial relations between objects as edges, while the question graph represents the dependencies between words via a dependency parser [141]. A recurrent unit [142] followed by an attention mechanism similar to cosine similarity with learnable transformations is used to process and align the two graphs for prediction. Instead of the language-irrelevant image-graph construction, Norcliffe *et al.* [143] use a graph learner to generate the image’s sparse graph representation conditioned on the question, followed by a graph CNN approach [24] to capture language-relevant spatial relations between objects in the image. Unlike previous methods to construct a static graph, Hu *et al.* [144] propose to generate a dynamic visual graph where the edges between objects are updated at each GNN-based message-passing iteration. The update is conditioned on the textual command vector extracted for each iteration (see Fig. 8). Jing *et al.* [145] follow a similar architecture to inference multiple questions for compositional VQA. Li *et al.* [146] propose generating three graphs for connecting semantic relation, spatial relation, and implicit relation between objects, respectively. GAT is utilized on each graph to assign different importance to nodes of the same neighborhoods and learn the relation-aware node representations. The outputs of GAT applied on the three graphs are aggregated to predict the answer. Instead of feature-based graph representation, Kim *et al.* [147] suggest using symbolic graphs to represent the image and question, generated through the scene graph parser [91] and dependency parser, respectively. Nodes of symbolic graphs present semantic units (*e.g.*, attributes and objects) with textual form, and edges present the relations (*e.g.*, predicates) between two units. The message passing neural network [148] is applied on the two graphs to get the informative representations and align the sub-graphs of the two symbolic graphs. Saqur *et al.* [149] further utilize the graph isomorphism network [150] to perform graph matching. The accuracy comparison of these GNN-based methods on the VQA v2.0 [151] and the GQA [152] datasets are shown in Tab. 4. In addition, the GNNs are applied to TextVQA [153] and visual commonsense reasoning [154], [155], which extend the VQA task by reading texts in images and enabling the commonsense reasoning, respectively.

**Fact-/Knowledge-based Visual Question Answering.** Compared to classical VQA, fact-based VQA [157] involves an external knowledge base of facts to conduct joint reasoning

Method	VQA v2.0 [151]		GQA [152]		
	std	dev	val	test-dev	test
Bottom-Up [156]	65.67	-	52.2	-	49.7
Graph Learner [143]*	66.18	-	-	-	-
single-hop + LCGN [144]*	-	-	63.9	55.8	56.1
Jing <i>et al.</i> [145]*	-	-	-	-	59.6
ReGAT [146]*	70.58	70.27	-	-	-
HANs [147]*	-	69.10	-	69.5	-

TABLE 4: Accuracy on two datasets for visual question answering. GNN-based methods are marked with \*.

with the image and question. A corresponding supporting fact is required to predict the answer for a pair of image and question. Narasimhan *et al.* [158] proposed first parsing and retrieving relevant facts from the external knowledge base using the image and question, and the retrieved facts are used to construct a fact graph. Then, they utilize a GCN to perform reasoning over facts to identify the supporting fact and answer. In addition to fact-based VQA, Singh *et al.* [159] proposed extending the classical gated GNNs [160] to integrate information from the knowledge base, question and image for knowledge-enabled VQA. They further utilize the knowledge base to more accurately recognize the texts in the image for VQA. Marino *et al.* [161] construct a symbolic-based knowledge graph from the knowledge base and perform explicit reasoning on the graph via relational GCN [162]. Then, the results of the explicit reasoning and the Transformer-based implicit reasoning are combined for answer prediction.

**Video Question Answering.** Similar to [140] in VQA, Park *et al.* [163] propose to represent the question as a parse question graph. To capture the temporal interactions in the video, they also construct a frame-based appearance graph and a motion graph. Then, GCNs [17] are used to learn the question-to-appearance and question-to-motion interactions on the three graphs. Unlike previous methods that use GNNs to learn relation-embedded node representations, Yu *et al.* [164] utilize GNNs to adaptively propagate the predicted probabilities between samples in the video to get consistent results between samples with high visual similarities. Instead of the frame or motion-level information, some works [165], [166] suggest constructing object-level visual graphs. In particular, Liu *et al.* [165] propose to combine GNNs and memory networks [167] to perform dynamic relation reasoning on visual and semantic graphs at the object level.

## 5.2 Visual Grounding

Visual grounding aims to locate the referent on an input image with respect to a natural language expression. Similar to the VQA task, GNNs here are introduced to capture the dependencies in visual and linguistic components.

**Referring Expression Grounding.** As shown in Fig. 9, Yang *et al.* [168] propose constructing a language-guided visual relation graph to represent the image conditioned on the expression. Then, they apply gated GCNs on the graph to learn visual-linguistic fusion and capture multi-order semantic context. Yang *et al.* [169] follow the same graph construction [168] but perform dynamic graph attention and convolution on the graph to achieve stepwisely graph reasoning under the guidance of linguistic structure. Similar to [169], Hu *et al.* [144] also generate the dynamic visual graph conditioned on language to capture the complex relations. Unlike some

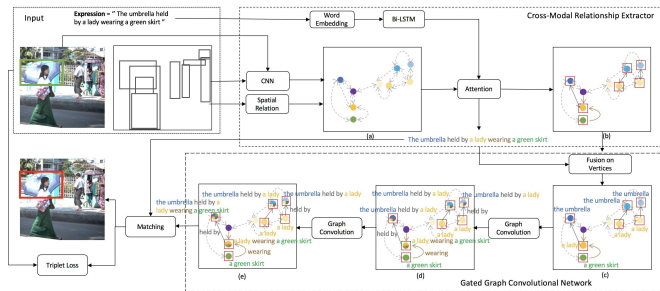


Fig. 9: Cross-Modal Relationship Inference Network (Figure used courtesy of [168]).

works [168], [170] considering multi-order relations, Wang *et al.* [171] consider direct intra-relations and inter-relations between neighboring objects to form a visual graph. They use language-guided graph attention and aggregation to update the node features that adapt to the expression. Different from previous methods, Chen *et al.* [172] propose constructing a multi-modal graph with random initialized bounding boxes as nodes and the semantic relations between most nearby neighboring nodes as edges. They utilize GAT to update node features and bounding boxes and introduce a graph Transformer to prune the nodes and edges iteratively. In addition, the GNNs [17], [123] have been utilized for referring expression segmentation [173], [174] and 3D visual grounding on point clouds [175] in a similar manner as for referring expression grounding.

**Phrase Grounding.** Phrase grounding aims to locate the referent in the image for each phrase in the expression. The referent of one phrase may be dependent on the referents of other phrases. Bajaj *et al.* [176] first construct a phrase graph, where nodes correspond to noun phrases and edges connect pairs of noun phrases, and then apply gated GNNs [160] to capture the dependencies between phrases. Moreover, they also perform a similar graph computation on a visual graph and a visual-linguistic fusion graph to jointly predict the referent for each phrase node. Different from the phrase graph construction in [176], Yang *et al.* [177] construct a language scene graph based on the dependency parsing of the expression, with noun phrases as nodes and relations between phrases as edges. They develop a one-stage graph-based propagation network for phrase grounding. The works [178], [179] use the same language scene graph in [177] and apply GCNs and attention mechanism on the graph to learn visual features corresponding to the graph nodes. In addition to the language scene graph, [180] construct a visual scene graph [181] and extended the standard GCNs to learn disentangled node representations over various motifs on the graphs and capture motif-aware context.

**Video Grounding.** Video grounding require grounding the expression in a video to obtain the temporal boundaries or the referred object's spatio-temporal tube. It is vital to capture the temporal or spatio-temporal correlation for video grounding. Zhang *et al.* [182] construct a spatial relation graph over objects in each frame and a temporal dynamic graph where nodes correspond objects in all frames and edges connect the same objects in consecutive frames. Then, they fuse the language representation into the two graphs and utilize graph convolution to capture the spatio-temporal correlation on the graphs. Zhao *et al.* [183] develop a different

way of constructing the temporal graph where each node represents an interval, and each direct edge represents the overlapping relation between two intervals. The GNNs [184] are adopted for passing messages on the graph. In addition, Li *et al.* [185] have utilized GNNs for compositional temporal grounding. The cross-graph GNNs are used to capture the hierarchical semantic correlations among global events, local actions, and atomic objects of the video and sentence.

### 5.3 Image Captioning

**Image Captioning.** Image captioning is the task of generating a complete and natural description for an image. The relations between objects in the image are natural priors to describe the image. Yao *et al.* [186] construct a semantic graph and a spatial graph to represent objects with their semantic and spatial relation types. Then, they extend the GCNs [17] on the graphs to obtain object representations with the inherent visual relations and use the attention LSTM [187] to decode the captioning based on the object representations. Yao *et al.* [188] use the same graph construction and GCNs as in [186] and extend the single object-level relation modeling into three hierarchical levels of the image, regions and objects. Unlike previous works only capturing the visual relations, Yang *et al.* [189] use the GCNs and sentence reconstruction to capture the language inductive bias to form a dictionary at the training stage. At the inference stage, they utilize the attention between the image scene graph and the dictionary to embed the language inductive bias into visual representations. Unlike previous methods directly decoding the GNN-based context representations of the image scene graph to sentence, [190] decompose the scene graph into a set of sub-graphs and select important sub-graphs to decode at each time step. To achieve a user desired captioning and enrich the diversities in a fine-grained level, Chen *et al.* [191] propose using an abstract scene graph to control the described objects, attributes, and relations in the captioning. The multi-relational GCN [162] is used to encode the abstract scene graph grounded in the image. Nguyen *et al.* [192] propose combining the image scene graph with a human-object interaction graph extracted from [193] to enhance the salient parts of the scene graph. Then, they follow the similar GCN-LSTM architecture in [186] to generate the sentence.

**Video Captioning.** Video captioning requires generating the description according to a given video. To learn the interaction between objects over time, Zhang *et al.* [194] construct an object relation graph to connect each object to top-k corresponding objects in all frames and use GCNs to learn the relation message passing on the graph. Like image captioning, they generate the description corresponding to the relational object features via an attention LSTM [187]. With the same motivation as [194], Pan *et al.* [195] construct a spatio-temporal graph and adopt GCNs to update node features. For the graph construction, they first take objects in single frames as nodes and normalized IOU between objects as edge weights, then connect semantically similar objects in two consecutive frames. Contrary to previous GCN-LSTM architectures, Chen *et al.* [196] propose aggregating the information in the temporal graph and feed the aggregation result into the LSTM decoder, which adjusts the graph structure conditioned on its hidden state and also updates the hidden state according to the graph representation.

### 5.4 Others

**Image-Text Matching.** Image-text matching aims to measure the visual-semantic similarity for a pair of image and sentence, which serves a vital role in visual-linguistic cross-modal retrieval. Since the local similarity between regions and words contributes to the global visual-semantic similarity, Huang *et al.* [197] propose utilizing the cross-modal GCNs to align the visual regions and word representations for global similarity computation. Different from [197], Li *et al.* [198] propose first learning relation-enhance global image representation based on the local regions and their relations, and then matching the global image representation with the sentence representation. The GCNs are used to perform relation reasoning on image regions to generate the relation-enhance features. Similar to [198], Yan *et al.* [199] also use GCNs to reason on semantic relations between image regions. In addition, they propose a discrete-continuous policy gradient algorithm to transform the visual and text modality into a common space. Wang *et al.* [200] improve the region-based relation reasoning by introducing commonsense knowledge to the reasoning process. They construct a concept correlation graph and learn consensus-aware concept representations via stacked GCN layers. Besides constructing a relation graph on image regions, Liu *et al.* [201] and Li *et al.* [202] build a textual graph of the sentence via a dependency parser and perform the semantically matching between the two graphs via the GCNs and attention mechanism. In addition to image-text matching, the GNNs have been utilized for video-text matching [203], [204], [205].

**Vision-Language Navigation.** Vision-language navigation requires an agent to navigation in unseen environment following a natural language instruction [206]. Deng *et al.* [207] develop an evolving graphical planner model, which iteratively and dynamically expands the trajectory graph built on the visited nodes, current node, the potential action nodes and their relations and performs the GNNs on the graph to predict the current action. Unlike [207], Chen *et al.* [208] use the GNNs to capture visual appearance and connectivity in the environment from the environment’s topological map. Gao *et al.* [209] propose involving external knowledge in the action prediction and performing the GCNs on the external and internal environment knowledge graphs to extract external knowledge for cooperating with internal knowledge. Chen *et al.* [210] propose generating a layout graph at each step conditioned on the instruction and using graph convolution to learn the current navigation state from the current layout graph and history layout memory. The navigation state is used to predict the action probability distribution at the current step. Similar to [207], Chen *et al.* [211] construct the environment graph on visited, navigable, and current nodes. Furthermore, they aggregate the graph into the self-attention between nodes to predict the navigation score for each node.

### 5.5 Discussion

Natural language sentences contain natural dependency structures, while images can take the form of spatial, semantic, or scene graph representations. GNNs thus are utilized naturally by the vision-and-language community to capture the relations among visual, linguistic, or multi-modal



TABLE 5: Overall Accuracy (oAcc.) on the ModelNet40 dataset for point cloud classification.

Method	Reference	oAcc.
PointGrid [244]	CVPR'18	92.0
PointCNN [214]	NeurIPS'18	92.2
PointConv [215]	CVPR'19	92.5
SpecGCN [227]	ECCV'18	92.1
SpiderCNN [245]	ECCV'18	92.4
DGCNN [246]	TOG'19	92.9
DeepGCN [27]	ICCV'19	93.6
Point Transformer [34]	ICCV'21	93.7

### 6.1.2 Mesh Representation

The polygonal mesh discretely represents the surface of a 3D shape with faces and vertices. Since it can be viewed as an undirected graph, mainstream GNNs or graph Transformers can be used for 3D mesh analysis [247], [248], [249], [250], [251], [252], [253], [254], [255], [256], [257], [258], [259].

A line of works explore graph convolution on different components, *e.g.* edges [247], facets [248], both edges and vertices [260], and learned features [250]. In MeshCNN [247], graph convolution and pooling operations are defined on the edges of a triangular mesh, as illustrated in Fig. 11. Differently, MeshNet [248] introduces convolution on mesh facets and feature splitting to obtain spatial and structural mesh features. MeshSNet [249] performed graph-constrained learning on 3D dental surfaces. DCM-Net [260] performs graph-based operations on both edges and vertices by jointly exploiting geodesic and Euclidean convolutions, which encourages context information flow within either spatially or geodesically nearby patches. PD-MeshNet [252] constructed a primal and a dual graph on an input 3D mesh to connect the features from mesh faces and vertices respectively, then employed Graph Attention Networks to dynamically aggregate these features. Compared with the static way of graph construction on edges, vertices, or facets, FeaStNet [250] constructs dynamic correspondences between filter weights and graph neighborhoods with arbitrary connectivity that is learned in the feature space.

Besides, SpiralNet++ [251] presents a fast and efficient intrinsic mesh convolution operator that improves [261] by fusing neighboring node features with local geometric structure information at multiple scales. A stacked dilated mesh convolution block is proposed in [253] that can inflate the receptive field of graph convolution kernels. PolyNet [254] designs a specific polygon mesh representation with a multi-resolution structure, and two operations, polynomial convolution and pooling, invariant to the number of adjacent vertices, their permutations, and their pairwise distances in local patches. He *et al.* [255] further introduce differential geometry to improve graph convolutional operation on 3D mesh, through learning direction sensitive geometric features from mesh surfaces. GET [256] borrow the attention mechanism in Graph Attention Network to build an efficient Transformer architecture with both gauge equivariance and rotation invariance on triangle meshes.

More recently, SubdivNet [257] performs representation learning on meshes with loop subdivision sequence connectivity by constructing hierarchical mesh pyramids. Laplacian2Mesh [258] considers the graph convolution and pooling on triangular meshes in the spectral domain, which

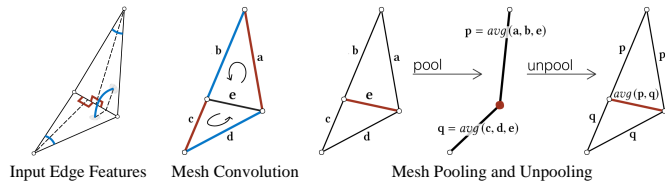


Fig. 11: MeshCNN (Figure used courtesy of [247]).

maps the mesh features in the Euclidean space to the multi-dimensional Laplacian-Beltrami space. Different from the custom of constructing graphs with regular neighborhood structures, MeshWalker [259] applies a similar way as in [224] to mesh analysis, where random walks along edges are conducted for 3D shape information extraction. AttWalk [262] enhances MeshWalker by exploring the meaningful interactions among different walks.

## 6.2 3D Understanding

GNNs are powerful methods for high-quality representation learning of both local and global regions, which leads to accurate context-aware semantic understanding. 3D understanding tasks with popular GNN applications include 3D segmentation, detection, and visual grounding. Based on GNN-based 3D representation learning approaches, the methods proposed for 3D understanding tasks further take the instance-level or/and scene-level features into consideration, where GNNs play an important role in learning inter-instance and contextual information.

### 6.2.1 3D Point Cloud Segmentation

3D point cloud segmentation (including semantic segmentation and instance segmentation) is a challenging task, where the algorithms need to understand not only the global semantics, but also the fine-grained point-wise signature.

Wang *et al.* [263] regard the individual objects as the subgraphs and cluster the indoor-scene scan using an anchor-guided graph matching method. Another early work by Yi *et al.* [229] focuses on shape part segmentation task, and try to share parameters across related but different shape graphs through synchronizing their spectral domains. Qi *et al.* [264] firstly construct large-scale semantic graph in 3D scenes to incorporate 3D geometric relations in a learning-based way. It starts from RGBD inputs and constructs k-nearest neighbor graphs upon the point clouds, and the semantic information from the image and the geometric information from the point cloud can be combined together through a graph neural network. SPG [265] constructs superpoint graph with rich contextual information, by dividing the whole point clouds into simple geometric partitions, for efficiently segmenting millions of points. Landrieu *et al.* [266] further propose graph-structured contrastive loss and cross-partition weighting strategy to better oversegment point clouds into superpoints in a supervised manner, which produced high contrast at objects' borders and compact representations in each body part. To better handle irregular data structures of point clouds, GACNet [267] performs graph attention convolution on local neighboring point sets, where the attention weights are learned from both 3D coordinates and point features, so that the network can attend most relevant neighboring points to better capture the 3D structure of the point cloud.

TABLE 6: Performance (mIoU) on the S3DIS Area-5 dataset for point cloud semantic segmentation.

Method	Reference	mIoU
TangentCConv [279]	CVPR'18	52.8
PointCNN [214]	NeurIPS'18	57.3
MinkowskiNet [280]	CVPR'19	65.4
PCCN [281]	CVPR'18	58.3
SPG [266]	CVPR'19	61.7
GACNet [234]	CVPR'19	62.9
Point Transformer [34]	ICCV'21	70.4
Fast Point Transformer [36]	CVPR'22	70.4
Stratified Transformer [37]	CVPR'22	72.0

PyramNet is equipped with a Graph Embedding Module [268] to strengthen the learning ability on local geometric details. DeepGCNs [27] adapt residual/dense connections and dilated convolutions into GCNs and trained very deep GCNs for 3D semantic segmentation. Jiang *et al.* [269] propose to hierarchically construct graphs, where a point branch and edge branch are interacted with each other. PointWeb [270] uses Adaptive Feature Adjustment (AFA) module to enhance the interaction between local points that are densely connected by graph structures. Combining depthwise graph convolution and pointwise convolution, HDGCN [271] customizes DGConv to extract local features on point clouds. Lei *et al.* [272] seek to build the local graph as a ball space around a center point, and split it into volumetric bins, where the weights of a neighboring point can be efficiently determined by its bin location. Ma *et al.* [273] designs Point Global Context Reasoning (PointGCR) module, which adopted relational reasoning to pass global context information among point nodes. Grid-GCN [274] employ Coverage-Aware Grid Query module and Grid Context Aggregation to significantly increase the speed during processing large-scale point cloud, while maintaining decent accuracy. RandLA-Net [275] takes advantage of the lightweight random sampling strategy and attentive graph pooling method to efficiently model the per-point semantics. Point2Node [276] explores the correlation among graph nodes from different scales. Xu *et al.* [277] introduce PAConv to dynamically model edge weights via assigning adaptive coefficients on several implicit basic kernels. SegGroup [278] applies GCNs to decrease the difference between the nodes from the same instances and increase the variance between the nodes of different instances, serving for both 3D semantic and instance segmentation tasks in a weakly-supervised manner. The performances of some of representative methods mentioned above on the point cloud semantic segmentation are listed in Tab. 6, which shows the superiority of GNN-based methods.

### 6.2.2 3D Object Detection

3D object detection drives many applications such as autonomous driving, robotic manipulation, and navigation. Object DGCNN [282] generalizes dynamic graph convolution to model scene-level 3D understanding for the object detection task. To better handle the sparsity in the observations and the spatially-discrete features in camera view images, Liang *et al.* [283] improved deep parametric continuous convolution [281], which computes dynamic convolution

kernel weights, to connect points in different modalities. Geo-CNN [284] performs convolutions on local spherical neighborhood graphs during the 3D object detection task. Jesus *et al.* [285] then formally introduce graph convolution networks to align object proposals on 3D LiDAR point clouds. HGNet [286] leverages graph convolution to extract point relationships hierarchically for better modeling relative object positions and shapes. Shi *et al.* [287] propose Point-GNN for one-stage 3D object detection, where the neighboring points within a fixed radius are connected in a graph, and an auto-regression method is designed to reduce the translation variance by dynamically refining point positions. Further, Feng *et al.* [288] build 3D object-object relationship graphs, where the relational reasoning between proposal features is performed in an end-to-end manner.

### 6.2.3 3D Visual Grounding

3D visual grounding aims to localize desired objects or areas in a 3D point cloud according to a descriptive linguistic sentence or phrase. It is usually formulated as a multi-modal instance matching problem, where multiple objects are detected from the 3D scene and matched against the description. Graph is one of the popular alternatives to represent the relations among visual or textual objects so that graph neural networks can be applied to extract object features with rich relation information [289], [290], [291]. TGNN [289] proposes to use a GNN in the referring stage for computing the matching score between the query and each segmented instance. InstanceRefer [290] models the relations among instances and adopts a DGCNN for feature extraction. Feng *et al.* [291] represent both 3D visual scenes and textual queries as graphs, and a graph attention module is used for context-aware feature refinement.

### 6.2.4 Discussion

GCN-based methods are the most popular solutions for point cloud understanding, where both local point neighborhoods and global contextual information should be modeled. Recent works [34], [35] proposed Transformer architectures for stronger feature extraction via the self-attention mechanism but at the cost of efficiency. However, the problem of a good combination of graph convolution and self-attention for 3D understanding has been less explored, with a very recent work 3DCTN [238] adopting graph convolution for efficient local feature extraction and self-attention for global interaction modeling. A future direction would be a comprehensive framework that performs point-neighborhood-level, instance-level, and scene-level understanding, and leverages the complementary advantages of MLP, graph convolution, and self-attention to achieve a balance between efficiency and performance.

## 6.3 3D Generation

In 3D generation, GNNs are widely adopted to (i) learn the required manipulation to the 3D input, *e.g.*, adjusting point positions for the task of point cloud denoising; (ii) generate a 3D shape given a target reference, *i.e.*, 3D reconstruction. In general, GNNs in 3D generation tasks develop from using graph convolutions only to further incorporating graph attention, and finally to graph Transformer, which seamlessly exploits the advantages of both structures.

### 6.3.1 Point Cloud Completion and Upsampling

The scanned data from 3D sensors are usually sparse, non-uniform, and incomplete. Point cloud completion and upsampling aim to produce complete and dense point clouds from real scans. The challenge lies in the recovery of complete object structure from noisy points. A two-stage framework is proposed in ECG [292], by exploiting skeleton as the intermediate product for structure representation and developing a hierarchical encoder based on graph convolution to extract multi-scale edge features. In [293], Leap-type EdgeConv [123] is used to capture local geometric features and a cross-cascade module to hierarchically combine local and global features. Shi *et al.* [294] regard point cloud completion as a generation task and cast the input data and intermediate generation as controlling and supporting points, and a graph convolution network is utilized to guide the optimization process. For the task of upsampling, a multi-step point cloud upsampling network is proposed in [295] to compute the K-nearest neighborhood for feature aggregation. Different from PU-GCN [296] that integrates densely connected graph convolution into an Inception module, AR-GCN [297] incorporates residual connections into GCN to exploit the correlation between point clouds of different resolutions, as well as a graph adversarial loss to capture the characteristic of high-resolution ones. PUGeo-Net [298] extends DGCNN by adding two modules for feature recalibration and point expansion.

### 6.3.2 3D Data Denoising

Given that the denoising task is mostly concerned with local representations of point neighborhoods, a straightforward application of GCN (*e.g.* DGCNN [123]) suffers from instability [299]. To solve this issue, DMR [300] builds on DGCNN [123] to learn the underlying manifold of the noisy input from differentially subsampled points and their local feature for less perturbation. GPDNet [299] proposes to build hierarchies of local and non-local features to regularize the underlying noise in the input point cloud. For 3D mesh denoising, Armando *et al.* develop a multi-scale graph convolutional network in [301] that built on CNN-based image denoising techniques. More recently, GCN-Denoiser [302], presents a rotation-invariant graph representation for local surface patches and performs graph convolution on both static graph structures in the local patch and dynamic learnable structures. GeoBi-GNN [303] excavates the dual-graph structure in meshes to capture both the position and normal noise through a U-Net architecture based on GNN.

### 6.3.3 3D Reconstruction

**Point Cloud Generation.** FoldingNet [304] develops a graph-based auto-encoder to deform a 2D grid into a point cloud with delicate structures. In [305], a unified latent space is constructed on graph representation, with a graph network, StructureNet, to encode or generate continuous representations like point clouds or discrete ones like images. Inspired by the success of GANs some works [306], [307], [308] focus on unsupervised point cloud generation from a random code sampled from a pre-defined distribution. The [306] studies the unsupervised graph-convolutional generator in GAN that can extract localized features from point clouds. TreeGAN [307] proposes a GAN model based on tree-structured

graph convolution. HSGAN [308] transforms the random code into a graph representation based on a hierarchical GCN and incorporates a self-attention mechanism into GAN. **Mesh Generation.** Pixel2Mesh [309] first employs GNNs for mesh reconstruction from single images. Instead of learning a direct mapping from images to meshes, Pixel2Mesh++ [310] use GCN to predict a series of deformations to refine the coarsely generated shape, targeting on multi-view mesh reconstruction. Mesh R-CNN [311] considers reconstruction from images with multiple objects. It augments Mask R-CNN [312] with 3D shape inference, where a GCN is developed for mesh refinement from a coarse cubified one. Vox2Mesh [313] directly addresses the task of mesh reconstruction from image volumes with a GCN in the decoder to refine a sphere mesh to match the target shape. As a more editable input, scene graphs are considered in [314] to generate and manipulate 3D scene meshes. A GCN-based variational auto-encoder is introduced in [314] to generate both the target object shapes in a scene and their corresponding layout, and the input scene graph naturally allows for semantic control on the generation. In addition, Mesh Graphormer [38] introduces the graph Transformer structure for human mesh reconstruction via combining graph convolution and self-attention for learning both local and global features.

**Human-related Mesh Reconstruction.** For human body reconstruction, Kolotouros *et al.* [315] improve the template-based mesh regression approach through a GCN to explicitly encode the template mesh structure and combine image features for regression. A bilayer graph is designed in [316] to represent the fine shape and human pose simultaneously, and a GCN is applied as the encoder to jointly perform pose estimation and mesh regression. DC-GNet [317] takes occlusion cases into account where human bodies are incomplete in images. For human body reconstruction, Pose2Mesh [318] builds on a GCN to estimate human mesh vertices' positions from 2D human pose. A lightweight graph Transformer is introduced in [319] for pose-guided mesh regression. Lin *et al.* [320] utilize GCN to generate high-fidelity face texture from a given image. A lightweight GCN-based subnetwork is proposed in [321] for face reconstruction. Besides, hand mesh reconstruction is also explored in [322] and [323].

### 6.3.4 Discussion

The most popular solutions for 3D generation tasks build on graph convolution [17], [123], which enables a network to effectively model local interactions. Recently, the self-attention mechanism is adopted for capturing global interactions [34], [38]. However, graph Transformers have not been adequately explored for 3D generation, *e.g.* general 3D object or scene reconstruction, and more graph Transformers are expected to be developed. In addition, in view of the large data size in 3D generation tasks, a practical direction would be promoting the efficiency of graph convolutional networks and graph Transformers.

## 7 MEDICAL IMAGE ANALYSIS

The applications of GNNs on medical image analysis include, but are not limited to, brain activity investigation, disease diagnosis, and anatomy segmentation.

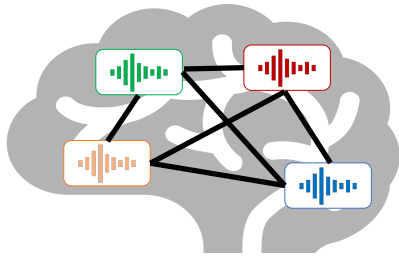


Fig. 12: Brain activity analysis using GNNs. Colors denote brain regions (nodes in GNNs) with different functions/structures, where the signal symbol stands for associated f-MRI data. Regions are connected through graph edges.

## 7.1 Brain Activity Investigation

As shown in Fig. 12, the brain can be divided into regions, and region responses and interconnections are interpreted for brain activity investigation.

### 7.1.1 Brain Signal Disorder Recognition

**Autism spectrum disorder (ASD).** Autism spectrum disorder is a type of developmental disorder that often adversely affects people’s social communication and interaction. Recently, GNNs have been employed to identify ASD in functional magnetic resonance imaging (f-MRI) [324], where in most cases, the node features consist of imaging features from different brain regions while the inter-region connections can be viewed as graph edges.

Parisot *et al.* [325] introduced spectral GCNs to conduct brain analysis in populations. The imaging feature of each subject serves as the vertex in the graph. The graph edge would be built if the similarity score of two subjects’ imaging and non-imaging (e.g., phenotypic data) features is above an artificially defined threshold. The proposed GCN framework outperforms the archetypical ridge classifier by at least 5% on different datasets. Anirudh *et al.* [326] addressed the instability problem in the step of population graph construction (with fewer edges) and introduced the bootstrap approach to construct an ensemble of multiple GCNs, which provides performance gains over [325]. Rakhimberdina and Murata [327] replaced the spectral GCNs in [325] with linear GCNs and optimized the edge construction step. Jiang *et al.* [328] proposed hybrid GCNs that maintain a hierarchical architecture to jointly incorporate information from both subject and population levels. Peng *et al.* [329] applied federated learning to train GCNs on inter-institutional data by first inpainting local networks with masked nodes and then training a global network across institutions.

Besides the population-based methods, Ktena *et al.* [330] used siamese GCNs to conduct distance metric learning on functional graphs of single subjects, outperforming the Principal Component Analysis (PCA) based baseline by over 10% on different imaging sites. Based on the work [330], Yao *et al.* [331] proposed triplet GCNs that contrast matching and non-matching functional connectivity graphs at the same time. In addition, multi-scale templates [331] were employed to advance the graph representation learning results. Li *et al.* [332] modified the ranking-based pooling methods by adding the regularization, enabling better node selection and prediction interpretation. In BrainGNN [333],

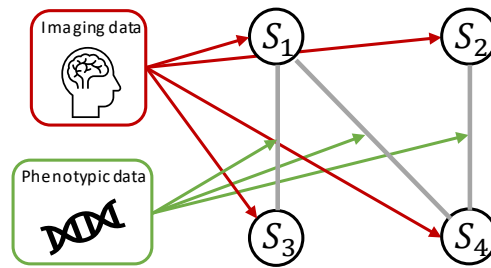


Fig. 13: Population-based brain disease diagnosis.  $S_i$  denotes the  $i$ -th subject.

ROI-aware graph convolution was introduced to encode the locality information into associated node embeddings. Kazi *et al.* [334] introduced inception GCN, which integrates spectral convolution with different kernel sizes to capture the intra- and inter-graph structural information.

**Other disorders.** Brain imaging can help distinguish patients with major depressive disorder (MDD) from normal ones. In [335], Yao *et al.* proposed an adaptive GCN framework to incorporate both spatial and temporal information from associated time-series f-MRI data. Yao *et al.* [336] aligned multi-index representations of f-MRI and encoded them into a shared latent feature space for making MDD predictions. For the diagnosis of bipolar disorder, Yang *et al.* [337] employed GAT networks and hierarchical pooling strategies to deal with variable-sized inputs. Rakhimberdina and Murata [327] applied linear GCNs to tackle the diagnosis issue of schizophrenia that is a mental illness related to the barrier of perceiving the reality.

### 7.1.2 Brain State Decoding

Zhang *et al.* [338] used deep graph convolution to interpret Resting-State Functional MRI (rsf-MRI) data into associated cognitive task results spanning six cognitive domains. In [339], the spatial-temporal graph convolution was employed to predict age and gender based on the BOLD signal of rsf-MRI data. Kim *et al.* [340] proposed to learn dynamic graph representations using spatial-temporal attention while Transformer serves as the encoder model to process a short sequence of brain connectome graphs.

## 7.2 Disease Diagnosis

In this section, we mainly review the related literature on diagnosis of brain and chest diseases using GNNs. Specifically, for brain diseases, we involve Alzheimer’s and Parkinson’s diseases as two representatives. As for chest pathologies, we do not restrict the type of disease.

### 7.2.1 Brain Disease Identification

**Alzheimer’s disease (AD).** Alzheimer’s disease is a type of neurodegenerative disease that gradually destroys brain cells. Parisot *et al.* [341] formulated the subject diagnosis issue as a graph labeling problem, where a spectral GCN was introduced to make diagnoses based on population analysis. As shown in Fig. 13, imaging data provide node features, while phenotypic data are interpreted as edge weights. The proposed approach surpasses previous state-of-the-arts by about 5% at least. Zhao *et al.* [342] used a GCN-based approach to detect Mild cognitive impairment (MCI) in AD.



In [343], Liu *et al.* deployed a GCN model to identify early mild cognitive impairment (EMCI, an early stage of AD) with a multi-task feature selection method on both imaging and non-imaging data. Yu *et al.* [344] designed a multi-scale GCN framework that integrates each subject’s structural information, functional information, and demographics (i.e., gender and age) for diagnosing EMCI based on population. Huang *et al.* [345] constructed an adaptive population graph with variational edges. The uncertainty of the adaptive graph was estimated using the proposed Monte-Carlo edge dropout [345]. Gopinath *et al.* [346] proposed a new graph pooling approach to analyze the geometrical changes of brain surface for improving AD diagnosis results using subject-specific information only. Ma *et al.* [347] incorporated local and global attention modules into GNNs. Besides, an attention-guided random walk strategy [347] was applied to extract features from dynamic graphs (with variable-sized nodes). Wee *et al.* [348] developed a cortical GNN model to take into account the cortical geometry and thickness information for identifying AD or MCI.

**Parkinson’s disease (PD).** Zhang *et al.* [349] implemented a multi-modal GCN model that fuses different brain image modalities for distinguishing PD from the healthy control, outperforming traditional diagnosis machine learning models by large margins. Kazi *et al.* [350] developed a LSTM-based attention mechanism to learn subject-specific features by ranking multi-modal features, and the fused representation was used for making final decisions. In [351], an end-to-end deep GCN framework was introduced to encode the cross-modality relationship into the graph while learning the mapping from structures to brain functions.

### 7.2.2 Chest Disease Analysis

Yu *et al.* [352] treated each CT scan as a node and connected nodes that share highest similarities. Features extracted from CNNs are passed to a one-layer GCN to help capture the relationship between similar samples. Similarly, Wang *et al.* [353] proposed to fuse image-level and relation-aware features via a GCN. Here, the GCN model is used to gather neighborhood information for deciding whether the input CT scan has COVID-19 or not. Zhang *et al.* [354] built a knowledge graph of chest abnormality based on prior knowledge on chest findings. The obtained graph was integrated with a graph embedding module, which was appended to a off-shelf CNN feature extractor. The output features of the graph embedding module can be used for both disease classification and radiology report generation. Hou *et al.* [355] pre-trained the label co-occurrence graph on radiology reports and integrated the resulting label embeddings with image-level features. The fused representations are passed to the Transformer encoder and the following GCN layers for feature fusion. Liu *et al.* [356], [357] introduced an anatomy-aware GCN model for mammogram detection. The anatomy-aware framework mainly involves two modules: i) a bipartite GCN to model the intrinsic geometrical and structural relations of ipsilateral views. ii) an inception GCN to model the structural similarities of bilateral views. The proposed anatomy-aware GCNs not only achieved state-of-the-art results on mammogram classification but also provided interpretable diagnosis results. Lian *et al.* [358] proposed a series of relation modules to capture the relations

among thoracic diseases and anatomical structures. Chen *et al.* [359] proposed an instance importance-aware GCN for applying multi-instance learning to 3D medical diagnosis, which helps to learn complementary representations by exploiting importance- and feature-based topologies. Gong *et al.* [360] introduced a graph context module for better bone age assessment by leveraging the whole hand’s growth pattern. Zhao *et al.* [361] proposed a general attribute-based medical image diagnosis framework by coupling probabilistic reasoning (Bayesian network) and neural reasoning (GCN) modules to model the causal relationships between attributes and diseases.

## 7.3 Anatomy Segmentation

Based on the segmentation targets, we roughly divide GNN-based segmentation approaches into three groups: brain surface segmentation, vessel segmentation, and other anatomical structure segmentation.

### 7.3.1 Brain Surface Segmentation

Cucurull *et al.* [362] exploited GCNs and GATs for mesh-based cerebral cortex segmentation. They found that either GCNs or GATs can obviously outperform traditional mesh segmentation approaches, sometimes by over 5%. Gopinath *et al.* [363] used GCNs to learn spectral embeddings directly in a space defined by surface basis functions for brain surface parcellation. Specifically, the proposed GCN model employs spectral filters to handle intrinsic surface representations, which were also validated in the task of brain parcellation. To better handle impaired topology, Wu *et al.* [364] proposed to directly conduct surface parcellation on top of the cortical manifold with the help of GCNs, which produced satisfactory results on surfaces that violate the spherical topology. He *et al.* [365] used the spectral graph Transformer to align multiple brain surfaces in the spectral domain, outperforming traditional GCN-based models by observable margins.

### 7.3.2 Vessel Segmentation

Wolterink *et al.* [366] used graph convolutional networks (GCNs) to forecast the spatial placement of vertices in a tubular surface mesh that divides the coronary artery lumen. Zhai *et al.* [367] combined GCNs with CNNs to categorize pulmonary vascular trees into either arteries or veins. In practice, the hybrid vessel segmentation model is trained on constructed vessel graphs, where the label of each node is whether it belongs to the artery class or the vein. Shin *et al.* [368] proposed a unified model that consists of both CNNs and GNNs to leverage graphical connectivity for vessel segmentation. Specifically, the unified framework exploits local and global information from perspectives of appearances and structures, respectively. Noh *et al.* [369] extracted vessel connectivity matrices from fundus and fluorescein angiography images via a hierarchical GNN, which were used to assist the classification of retinal artery/vein classification. To tackle high variations in intracranial arteries, Chen *et al.* [370] introduced a GNN segmentation model and a hierarchical refinement module to integrate structural information with relational prior knowledge for the segmentation of intracranial arteries. Considering vessels in 3D images often have diverse sizes and shapes, Yao *et al.* [371] proposed

a GCN-based point cloud network to incorporate the tubular prior knowledge into vessel segmentation, which not only helps to capture the global shape but also the local vascular structure. Yang *et al.* [372] introduced a partial-residual GCN to take into account both position features of coronary arteries and associated imaging features to conduct automated anatomical segmentation. Zhang *et al.* [373] integrated the intra-artery relation with the inter-organ dependencies for capturing anatomical dependencies. Zhao *et al.* [374] proposed a cascaded deep neural network, where cross-network multi-scale feature fusion is performed between a CNN-based U-Net and a graph U-Net to effectively support high-quality vessel segmentation.

### 7.3.3 Segmentation of Other Anatomical Structures

Selvan [375] proposed to use a GNN-based auto-encoder to learn node features for airway extraction while a decoder was employed to predict edges between nodes. Garcia-Uceda Juarez *et al.* [376] modified UNet [377] by replacing the convolution layers in the bottleneck with graph convolution layers, which helps encode the node connectivity into latent embeddings. The resulting hybrid UNet outperformed the classic UNet in the task of airway segmentation. In [378], a GNN-based graph refinement module was derived for to extract airway structures more accurately. Mukul *et al.* [379] formulated the post-processing procedure in pancreas and spleen segmentation as a semi-supervised graph labeling problem and proposed a GCN-based refinement strategy to replace the classic conditional random fields (CRFs) for segmentation mask post-processing. Tian *et al.* [380] applied GCNs to the interactive segmentation problem of prostate, where GCNs were responsible for refining the coarse contour produced by CNNs. Meng *et al.* [381], [382] developed a hybrid U-shape model for optic cup/disc segmentation, where the encoder consists of convolution layers while the decoder comprises graph convolution layers. The encoder and decoder is connected via attention modules, which help the decoder to leverage the more location information from the convolutional encoder. Chao *et al.* [383] presented a GNN that incorporates the global spatial priors of lymph node tumor into its learning process to further model the relations between lymph nodes. Yan *et al.* [384] first transform 3D MRI images into supervoxels, which were then passed to graph convolution layers to capture interconnections for brain tissue segmentation.

## 7.4 Discussion

Graph representation learning is the core idea behind GNN-based brain signal analysis, while self-supervised learning has been shown to improve the generalization ability of representations in medical imaging [385], [386], [387], [388]. Therefore, it is promising to incorporate self-supervised learning into existing GNN-based analysis frameworks. For instance, neighboring nodes can be contrasted with non-neighboring ones to learn invariant and discriminative node features using noise-contrastive estimation [389].

Multi-disease graphs are necessary for capturing inter-disease relations to achieve reliable diagnoses. For example, a knowledge graph [390], [391] can be integrated into a hierarchical multi-disease diagnosis system, where each node includes both imaging and non-imaging features of a specific

disease. The knowledge graph can be built using domain knowledge or clinical descriptions associated with images (such as radiology reports [392], [393], [394]).

GNN-based approaches resort to building graphs for encoding relations into latent representations. In practice, these graphs can be incorporated into label-efficient learning to assist medical image segmentation with limited annotations. For instance, we can apply GNNs to aggregate the representations of neighboring classes with rich annotations to improve the representations of rare diseases. Moreover, conducting graph-based reasoning [395] within GNN-based segmentation frameworks is also a promising direction, which helps improve the performance of segmentation models on unseen organs and diseases.

## 8 CONCLUSIONS

Despite the ground-breaking progress in perception, how to endow deep learning models with reasoning ability remains a formidable challenge for modern computer vision systems. In this regard, GNN and graph Transformers have demonstrated significant flexibility and superiority in dealing with ‘relational’ tasks. To this end, we have presented the first comprehensive survey of GNN and graph Transformers in computer vision from a task-oriented perspective. Specifically, a variety of classical and up-to-date algorithms are grouped into five categories according to the modality of input data, such as image, video, and point cloud. By systematically sorting out the methodologies for each task, we hope that this survey can shed light on more progress in the future. By providing discussion regarding key innovations, limitations, and potential research directions, we hope that readers can obtain new insights and go a further step towards human-like visual understanding.

## REFERENCES

- [1] Y. LeCun, Y. Bengio, and G. Hinton, “Deep learning,” *nature*, vol. 521, no. 7553, pp. 436–444, 2015.
- [2] A. Krizhevsky, I. Sutskever, and G. E. Hinton, “Imagenet classification with deep convolutional neural networks,” in *NeurIPS*, 2012.
- [3] K. He, X. Zhang, S. Ren, and J. Sun, “Deep residual learning for image recognition,” in *CVPR*, 2016.
- [4] M. Tan and Q. Le, “Efficientnet: Rethinking model scaling for convolutional neural networks,” in *ICML*, 2019.
- [5] P. W. Battaglia, J. B. Hamrick, V. Bapst, A. Sanchez-Gonzalez, V. Zambaldi, M. Malinowski, A. Tacchetti, D. Raposo, A. Santoro, R. Faulkner *et al.*, “Relational inductive biases, deep learning, and graph networks,” *arXiv preprint arXiv:1806.01261*, 2018.
- [6] A. Sperduti and A. Starita, “Supervised neural networks for the classification of structures,” *IEEE Transactions on Neural Networks*, vol. 8, 1997.
- [7] Y. Guo, H. Wang, Q. Hu, H. Liu, L. Liu, and M. Bennamoun, “Deep learning for 3d point clouds: A survey,” *IEEE TPAMI*, vol. 43, 2020.
- [8] V. P. Dwivedi and X. Bresson, “A generalization of transformer networks to graphs,” *arXiv preprint arXiv:2012.09699*, 2020.
- [9] D. Chen, L. O’Bray, and K. Borgwardt, “Structure-aware transformer for graph representation learning,” in *ICML*, 2022.
- [10] Z. Wu, S. Pan, F. Chen, G. Long, C. Zhang, and S. Y. Philip, “A comprehensive survey on graph neural networks,” *IEEE TNNLS*, vol. 32, 2020.
- [11] J. Zhou, G. Cui, S. Hu, Z. Zhang, C. Yang, Z. Liu, L. Wang, C. Li, and M. Sun, “Graph neural networks: A review of methods and applications,” *AI Open*, vol. 1, 2020.

- [12] Y. Rong, T. Xu, J. Huang, W. Huang, H. Cheng, Y. Ma, Y. Wang, T. Derr, L. Wu, and T. Ma, "Deep graph learning: Foundations, advances and applications," in *Proceedings of the 26th ACM SIGKDD International Conference on Knowledge Discovery & Data Mining*, 2020, pp. 3555–3556.
- [13] F. Scarselli, M. Gori, A. C. Tsoi, M. Hagenbuchner, and G. Monfardini, "The graph neural network model," *IEEE transactions on neural networks*, vol. 20, 2008.
- [14] J. Bruna, W. Zaremba, A. Szlam, and Y. LeCun, "Spectral networks and locally connected networks on graphs," in *ICLR*, 2014.
- [15] M. Henaff, J. Bruna, and Y. LeCun, "Deep convolutional networks on graph-structured data," *arXiv preprint arXiv:1506.05163*, 2015.
- [16] M. Defferrard, X. Bresson, and P. Vandergheynst, "Convolutional neural networks on graphs with fast localized spectral filtering," *NeurIPS*, vol. 29, 2016.
- [17] T. N. Kipf and M. Welling, "Semi-supervised classification with graph convolutional networks," in *ICLR*, 2017.
- [18] R. Levie, F. Monti, X. Bresson, and M. M. Bronstein, "Cayleynets: Graph convolutional neural networks with complex rational spectral filters," *IEEE Transactions on Signal Processing*, vol. 67, no. 1, pp. 97–109, 2018.
- [19] R. Li, S. Wang, F. Zhu, and J. Huang, "Adaptive graph convolutional neural networks," in *AAAI*, 2018.
- [20] J. Atwood and D. Towsley, "Diffusion-convolutional neural networks," *Advances in neural information processing systems*, vol. 29, 2016.
- [21] M. Niepert, M. Ahmed, and K. Kutzkov, "Learning convolutional neural networks for graphs," in *ICML*, 2016.
- [22] W. Hamilton, Z. Ying, and J. Leskovec, "Inductive representation learning on large graphs," *NeurIPS*, vol. 30, 2017.
- [23] P. Veličković, G. Cucurull, A. Casanova, A. Romero, P. Lio, and Y. Bengio, "Graph attention networks," in *ICLR*, 2018.
- [24] F. Monti, D. Boscaini, J. Masci, E. Rodola, J. Svoboda, and M. M. Bronstein, "Geometric deep learning on graphs and manifolds using mixture model cnns," in *CVPR*, 2017.
- [25] W. Huang, T. Zhang, Y. Rong, and J. Huang, "Adaptive sampling towards fast graph representation learning," *Advances in neural information processing systems*, vol. 31, 2018.
- [26] K. Xu, C. Li, Y. Tian, T. Sonobe, K.-i. Kawarabayashi, and S. Jegelka, "Representation learning on graphs with jumping knowledge networks," *arXiv preprint arXiv:1806.03536*, 2018.
- [27] G. Li, M. Muller, A. Thabet, and B. Ghanem, "Deepgcns: Can gcns go as deep as cnns?" in *ICCV*, 2019.
- [28] Y. Rong, W. Huang, T. Xu, and J. Huang, "Dropedge: Towards deep graph convolutional networks on node classification," in *ICLR*, 2020.
- [29] G. Li, M. Müller, B. Ghanem, and V. Koltun, "Training graph neural networks with 1000 layers," in *ICML*, 2021.
- [30] Z. Ying, J. You, C. Morris, X. Ren, W. Hamilton, and J. Leskovec, "Hierarchical graph representation learning with differentiable pooling," *NeurIPS*, vol. 31, 2018.
- [31] Y. Ma, S. Wang, C. C. Aggarwal, and J. Tang, "Graph convolutional networks with eigenpooling," in *Proceedings of the 25th ACM SIGKDD international conference on knowledge discovery & data mining*, 2019, pp. 723–731.
- [32] H. Gao and S. Ji, "Graph u-nets," in *ICML*, 2019.
- [33] K. Han, Y. Wang, J. Guo, Y. Tang, and E. Wu, "Vision gnn: An image is worth graph of nodes," in *NeurIPS*, 2022.
- [34] H. Zhao, L. Jiang, J. Jia, P. H. Torr, and V. Koltun, "Point transformer," in *ICCV*, 2021.
- [35] M.-H. Guo, J.-X. Cai, Z.-N. Liu, T.-J. Mu, R. R. Martin, and S.-M. Hu, "Pct: Point cloud transformer," *Computational Visual Media*, vol. 7, pp. 187–199, 2021.
- [36] C. Park, Y. Jeong, M. Cho, and J. Park, "Fast point transformer," in *CVPR*, 2022.
- [37] X. Lai, J. Liu, L. Jiang, L. Wang, H. Zhao, S. Liu, X. Qi, and J. Jia, "Stratified transformer for 3d point cloud segmentation," in *CVPR*, 2022.
- [38] K. Lin, L. Wang, and Z. Liu, "Mesh graphormer," in *ICCV*, 2021.
- [39] A. Vaswani, N. Shazeer, N. Parmar, J. Uszkoreit, L. Jones, A. N. Gomez, Ł. Kaiser, and I. Polosukhin, "Attention is all you need," *NeurIPS*, vol. 30, 2017.
- [40] Z.-M. Chen, X.-S. Wei, P. Wang, and Y. Guo, "Multi-label image recognition with graph convolutional networks," in *CVPR*, 2019.
- [41] T. Chen, M. Xu, X. Hui, H. Wu, and L. Lin, "Learning semantic-specific graph representation for multi-label image recognition," in *ICCV*, 2019.
- [42] J. Lanchantin, A. Sekhon, and Y. Qi, "Neural message passing for multi-label classification," in *ECML-PKDD*, 2019.
- [43] X. Wu, Q. Chen, W. Li, Y. Xiao, and B. Hu, "Adahgnn: Adaptive hypergraph neural networks for multi-label image classification," in *ACM MM*, 2020.
- [44] J. Ye, J. He, X. Peng, W. Wu, and Y. Qiao, "Attention-driven dynamic graph convolutional network for multi-label image recognition," in *ECCV*, 2020.
- [45] R. You, Z. Guo, L. Cui, X. Long, Y. Bao, and S. Wen, "Cross-modality attention with semantic graph embedding for multi-label classification," in *AAAI*, 2020.
- [46] H. D. Nguyen, X.-S. Vu, and D.-T. Le, "Modular graph transformer networks for multi-label image classification," in *AAAI*, 2021.
- [47] J. Zhao, K. Yan, Y. Zhao, X. Guo, F. Huang, and J. Li, "Transformer-based dual relation graph for multi-label image recognition," in *ICCV*, 2021.
- [48] V. Garcia and J. Bruna, "Few-shot learning with graph neural networks," in *ICLR*, 2018.
- [49] Y. Liu, J. Lee, M. Park, S. Kim, E. Yang, S. J. Hwang, and Y. Yang, "Learning to propagate labels: Transductive propagation network for few-shot learning," in *ICLR*, 2019.
- [50] J. Kim, T. Kim, S. Kim, and C. D. Yoo, "Edge-labeling graph neural network for few-shot learning," in *CVPR*, 2019.
- [51] Y. Luo, Z. Huang, Z. Zhang, Z. Wang, M. Baktashmotlagh, and Y. Yang, "Learning from the past: Continual meta-learning via bayesian graph modeling," in *AAAI*, 2020.
- [52] L. Yang, L. Li, Z. Zhang, X. Zhou, E. Zhou, and Y. Liu, "Dpgn: Distribution propagation graph network for few-shot learning," in *CVPR*, 2020.
- [53] C. Chen, K. Li, W. Wei, J. T. Zhou, and Z. Zeng, "Hierarchical graph neural networks for few-shot learning," *TCSVT*, 2021.
- [54] T. Yu, S. He, Y.-Z. Song, and T. Xiang, "Hybrid graph neural networks for few-shot learning," in *AAAI*, 2022.
- [55] M. Kampffmeyer, Y. Chen, X. Liang, H. Wang, Y. Zhang, and E. P. Xing, "Rethinking knowledge graph propagation for zero-shot learning," in *CVPR*, 2019.
- [56] G.-S. Xie, L. Liu, F. Zhu, F. Zhao, Z. Zhang, Y. Yao, J. Qin, and L. Shao, "Region graph embedding network for zero-shot learning," in *ECCV*, 2020.
- [57] L. Liu, T. Zhou, G. Long, J. Jiang, and C. Zhang, "Attribute propagation network for graph zero-shot learning," in *AAAI*, 2020.
- [58] L. Liu, T. Zhou, G. Long, J. Jiang, X. Dong, and C. Zhang, "Isometric propagation network for generalized zero-shot learning," in *ICLR*, 2021.
- [59] M. Mancini, M. F. Naeem, Y. Xian, and Z. Akata, "Learning graph embeddings for open world compositional zero-shot learning," *IEEE TPAMI*, 2022.
- [60] S. Chen, Z. Hong, G. Xie, Q. Peng, X. You, W. Ding, and L. Shao, "Gndan: Graph navigated dual attention network for zero-shot learning," *IEEE TNNLS*, 2022.
- [61] X. Ma, T. Zhang, and C. Xu, "Gcan: Graph convolutional adversarial network for unsupervised domain adaptation," in *CVPR*, 2019, pp. 8266–8276.
- [62] X. Yang, C. Deng, T. Liu, and D. Tao, "Heterogeneous graph attention network for unsupervised multiple-target domain adaptation," *IEEE TPAMI*, 2020.
- [63] S. Roy, E. Krivosheev, Z. Zhong, N. Sebe, and E. Ricci, "Curriculum graph co-teaching for multi-target domain adaptation," in *CVPR*, 2021.
- [64] Y. Luo, Z. Wang, Z. Huang, and M. Baktashmotlagh, "Progressive graph learning for open-set domain adaptation," in *ICML*, 2020.
- [65] Z. Wang, Y. Luo, Z. Huang, and M. Baktashmotlagh, "Prototype-matching graph network for heterogeneous domain adaptation," in *ACM MM*, 2020.
- [66] H. Wang, M. Xu, B. Ni, and W. Zhang, "Learning to combine: Knowledge aggregation for multi-source domain adaptation," in *ECCV*. Springer, 2020.
- [67] C. Chen, J. Li, X. Han, X. Liu, and Y. Yu, "Compound domain generalization via meta-knowledge encoding," in *CVPR*, 2022.
- [68] L. Liu, W. Ouyang, X. Wang, P. Fieguth, J. Chen, X. Liu, and M. Pietikäinen, "Deep learning for generic object detection: A survey," *IJCV*, vol. 128, no. 2, pp. 261–318, 2020.
- [69] H. Hu, J. Gu, Z. Zhang, J. Dai, and Y. Wei, "Relation networks for object detection," in *CVPR*, 2018.

- [70] H. Xu, C. Jiang, X. Liang, L. Lin, and Z. Li, "Reasoning-rcnn: Unifying adaptive global reasoning into large-scale object detection," in *CVPR*, 2019.
- [71] H. Xu, C. Jiang, X. Liang, and Z. Li, "Spatial-aware graph relation network for large-scale object detection," in *CVPR*, 2019.
- [72] C. Chi, F. Wei, and H. Hu, "Relationnet++: Bridging visual representations for object detection via transformer decoder," *NeurIPS*, vol. 33, 2020.
- [73] Z. Li, X. Du, and Y. Cao, "Gar: Graph assisted reasoning for object detection," in *WACV*, 2020.
- [74] G. Zhao, W. Ge, and Y. Yu, "Graphfpn: Graph feature pyramid network for object detection," in *ICCV*, 2021.
- [75] C. Chen, J. Li, H.-Y. Zhou, X. Han, Y. Huang, X. Ding, and Y. Yu, "Relation matters: Foreground-aware graph-based relational reasoning for domain adaptive object detection," *IEEE TPAMI*, 2022.
- [76] C. Chen, J. Li, Z. Zheng, Y. Huang, X. Ding, and Y. Yu, "Dual bipartite graph learning: A general approach for domain adaptive object detection," in *ICCV*, 2021.
- [77] W. Li, X. Liu, and Y. Yuan, "Sigma: Semantic-complete graph matching for domain adaptive object detection," in *CVPR*, 2022.
- [78] C. Zhu, F. Chen, U. Ahmed, Z. Shen, and M. Savvides, "Semantic relation reasoning for shot-stable few-shot object detection," in *CVPR*, 2021.
- [79] L. Zhang, X. Li, A. Arnab, K. Yang, Y. Tong, and P. Torr, "Dual graph convolutional network for semantic segmentation," in *BMVC*, 2019.
- [80] Y. Chen, M. Rohrbach, Z. Yan, Y. Shuicheng, J. Feng, and Y. Kalantidis, "Graph-based global reasoning networks," in *CVPR*, 2019.
- [81] L. Zhang, D. Xu, A. Arnab, and P. H. Torr, "Dynamic graph message passing networks," in *CVPR*, 2020.
- [82] C. Yu, Y. Liu, C. Gao, C. Shen, and N. Sang, "Representative graph neural network," in *ECCV*, 2020.
- [83] X. Li, Y. Yang, Q. Zhao, T. Shen, Z. Lin, and H. Liu, "Spatial pyramid based graph reasoning for semantic segmentation," in *CVPR*, 2020.
- [84] H. Hu, D. Ji, W. Gan, S. Bai, W. Wu, and J. Yan, "Class-wise dynamic graph convolution for semantic segmentation," in *ECCV*, 2020.
- [85] C. Zhang, G. Lin, F. Liu, J. Guo, Q. Wu, and R. Yao, "Pyramid graph networks with connection attentions for region-based one-shot semantic segmentation," in *ICCV*, 2019.
- [86] G.-S. Xie, J. Liu, H. Xiong, and L. Shao, "Scale-aware graph neural network for few-shot semantic segmentation," in *CVPR*, 2021.
- [87] B. Zhang, J. Xiao, J. Jiao, Y. Wei, and Y. Zhao, "Affinity attention graph neural network for weakly supervised semantic segmentation," *IEEE TPAMI*, 2021.
- [88] Y. Wu, G. Zhang, Y. Gao, X. Deng, K. Gong, X. Liang, and L. Lin, "Bidirectional graph reasoning network for panoptic segmentation," in *CVPR*, 2020.
- [89] X. Wang, R. Girshick, A. Gupta, and K. He, "Non-local neural networks," in *CVPR*, 2018, pp. 7794–7803.
- [90] J. Yang, J. Lu, S. Lee, D. Batra, and D. Parikh, "Graph r-cnn for scene graph generation," in *ECCV*, 2018.
- [91] J. Johnson, R. Krishna, M. Stark, L.-J. Li, D. Shamma, M. Bernstein, and L. Fei-Fei, "Image retrieval using scene graphs," in *CVPR*, 2015.
- [92] G. Zhu, L. Zhang, Y. Jiang, Y. Dang, H. Hou, P. Shen, M. Feng, X. Zhao, Q. Miao, S. A. A. Shah *et al.*, "Scene graph generation: A comprehensive survey," *arXiv preprint arXiv:2201.00443*, 2022.
- [93] Y. Li, W. Ouyang, B. Zhou, J. Shi, C. Zhang, and X. Wang, "Factorizable net: an efficient subgraph-based framework for scene graph generation," in *ECCV*, 2018.
- [94] M. Qi, W. Li, Z. Yang, Y. Wang, and J. Luo, "Attentive relational networks for mapping images to scene graphs," in *CVPR*, 2019.
- [95] R. Li, S. Zhang, B. Wan, and X. He, "Bipartite graph network with adaptive message passing for unbiased scene graph generation," in *CVPR*, 2021.
- [96] M. Suhail, A. Mittal, B. Siddiquie, C. Broaddus, J. Eledath, G. Medioni, and L. Sigal, "Energy-based learning for scene graph generation," in *CVPR*, 2021.
- [97] X. Wang and A. Gupta, "Videos as space-time region graphs," in *ECCV*, 2018.
- [98] S. Yan, Y. Xiong, and D. Lin, "Spatial temporal graph convolutional networks for skeleton-based action recognition," in *AAAI*, 2018.
- [99] R. Zeng, W. Huang, M. Tan, Y. Rong, P. Zhao, J. Huang, and C. Gan, "Graph convolutional networks for temporal action localization," in *ICCV*, 2019.
- [100] M. Xu, C. Zhao, D. S. Rojas, A. Thabet, and B. Ghanem, "G-tad: Sub-graph localization for temporal action detection," in *CVPR*, 2020.
- [101] W. Wang, X. Lu, J. Shen, D. J. Crandall, and L. Shao, "Zero-shot video object segmentation via attentive graph neural networks," in *ICCV*, 2019.
- [102] X. Lu, W. Wang, M. Danelljan, T. Zhou, J. Shen, and L. V. Gool, "Video object segmentation with episodic graph memory networks," in *ECCV*, 2020.
- [103] Y. Ou, L. Mi, and Z. Chen, "Object-relation reasoning graph for action recognition," in *CVPR*, 2022.
- [104] J. Zhang, F. Shen, X. Xu, and H. T. Shen, "Temporal reasoning graph for activity recognition," *IEEE TIP*, vol. 29, 2020.
- [105] J. Gao, T. Zhang, and C. Xu, "I know the relationships: Zero-shot action recognition via two-stream graph convolutional networks and knowledge graphs," in *AAAI*, 2019.
- [106] J. Zhou, K.-Y. Lin, H. Li, and W.-S. Zheng, "Graph-based high-order relation modeling for long-term action recognition," in *CVPR*, 2021.
- [107] J. Wu, L. Wang, L. Wang, J. Guo, and G. Wu, "Learning actor relation graphs for group activity recognition," in *CVPR*, 2019.
- [108] J.-H. Pan, J. Gao, and W.-S. Zheng, "Action assessment by joint relation graphs," in *ICCV*, 2019.
- [109] L. Shi, Y. Zhang, J. Cheng, and H. Lu, "Two-stream adaptive graph convolutional networks for skeleton-based action recognition," in *CVPR*, 2019.
- [110] B. Li, X. Li, Z. Zhang, and F. Wu, "Spatio-temporal graph routing for skeleton-based action recognition," in *AAAI*, 2019.
- [111] M. Li, S. Chen, X. Chen, Y. Zhang, Y. Wang, and Q. Tian, "Action-structural graph convolutional networks for skeleton-based action recognition," in *CVPR*, 2019.
- [112] R. Zhao, K. Wang, H. Su, and Q. Ji, "Bayesian graph convolution lstm for skeleton based action recognition," in *ICCV*, 2019.
- [113] S. Hochreiter and J. Schmidhuber, "Long short-term memory," *Neural computation*, vol. 9, 1997.
- [114] L. Shi, Y. Zhang, J. Cheng, and H. Lu, "Skeleton-based action recognition with directed graph neural networks," in *CVPR*, 2019.
- [115] Z. Liu, H. Zhang, Z. Chen, Z. Wang, and W. Ouyang, "Disentangling and unifying graph convolutions for skeleton-based action recognition," in *CVPR*, 2020.
- [116] G. A. Sigurdsson, G. Varol, X. Wang, A. Farhadi, I. Laptev, and A. Gupta, "Hollywood in homes: Crowdsourcing data collection for activity understanding," in *ECCV*, 2016.
- [117] A. Shahroudy, J. Liu, T.-T. Ng, and G. Wang, "Ntu rgb+ d: A large scale dataset for 3d human activity analysis," in *CVPR*, 2016.
- [118] W. Kay, J. Carreira, K. Simonyan, B. Zhang, C. Hillier, S. Vijayanarasimhan, F. Viola, T. Green, T. Back, P. Natsev *et al.*, "The kinetics human action video dataset," *arXiv preprint arXiv:1705.06950*, 2017.
- [119] C. Si, W. Chen, W. Wang, L. Wang, and T. Tan, "An attention enhanced graph convolutional lstm network for skeleton-based action recognition," in *CVPR*, 2019.
- [120] B. Wu, A. Wan, X. Yue, P. Jin, S. Zhao, N. Golmant, A. Gholamnejad, J. Gonzalez, and K. Keutzer, "Shift: A zero flop, zero parameter alternative to spatial convolutions," in *CVPR*, 2018.
- [121] K. Cheng, Y. Zhang, X. He, W. Chen, J. Cheng, and H. Lu, "Skeleton-based action recognition with shift graph convolutional network," in *CVPR*, 2020.
- [122] K. Cheng, Y. Zhang, C. Cao, L. Shi, J. Cheng, and H. Lu, "Decoupling gcn with dropgraph module for skeleton-based action recognition," in *ECCV*, 2020.
- [123] Y. Wang, Y. Sun, Z. Liu, S. E. Sarma, M. M. Bronstein, and J. M. Solomon, "Dynamic graph cnn for learning on point clouds," *ACM TOG*, vol. 38, 2019.
- [124] C. Zhao, A. K. Thabet, and B. Ghanem, "Video self-stitching graph network for temporal action localization," in *ICCV*, 2021.
- [125] Y. Bai, Y. Wang, Y. Tong, Y. Yang, Q. Liu, and J. Liu, "Boundary content graph neural network for temporal action proposal generation," in *ECCV*, 2020.
- [126] Y. Huang, Y. Sugano, and Y. Sato, "Improving action segmentation via graph-based temporal reasoning," in *CVPR*, 2020.
- [127] G. Brasó and L. Leal-Taixé, "Learning a neural solver for multiple object tracking," in *CVPR*, 2020.

- [128] X. Weng, Y. Wang, Y. Man, and K. M. Kitani, "Gnn3dmot: Graph neural network for 3d multi-object tracking with 2d-3d multi-feature learning," in *CVPR*, 2020.
- [129] M. Li, S. Chen, Y. Zhao, Y. Zhang, Y. Wang, and Q. Tian, "Dynamic multiscale graph neural networks for 3d skeleton based human motion prediction," in *CVPR*.
- [130] T. Sofianos, A. Sampieri, L. Franco, and F. Galasso, "Space-time-separable graph convolutional network for pose forecasting," in *ICCV*, 2021.
- [131] Y. Cai, L. Ge, J. Liu, J. Cai, T.-J. Cham, J. Yuan, and N. M. Thalmann, "Exploiting spatial-temporal relationships for 3d pose estimation via graph convolutional networks," in *ICCV*, 2019.
- [132] A. Mohamed, K. Qian, M. Elhoseiny, and C. Claudel, "Social-stgcn: A social spatio-temporal graph convolutional neural network for human trajectory prediction," in *CVPR*, 2020.
- [133] C. Yu, X. Ma, J. Ren, H. Zhao, and S. Yi, "Spatio-temporal graph transformer networks for pedestrian trajectory prediction," in *ECCV*, 2020.
- [134] J. Sun, Q. Jiang, and C. Lu, "Recursive social behavior graph for trajectory prediction," in *CVPR*, 2020.
- [135] L. Shi, L. Wang, C. Long, S. Zhou, M. Zhou, Z. Niu, and G. Hua, "Sgcn: Sparse graph convolution network for pedestrian trajectory prediction," in *CVPR*, 2021.
- [136] L. Li, M. Pagnucco, and Y. Song, "Graph-based spatial transformer with memory replay for multi-future pedestrian trajectory prediction," in *CVPR*, 2022.
- [137] S. Antol, A. Agrawal, J. Lu, M. Mitchell, D. Batra, C. L. Zitnick, and D. Parikh, "Vqa: Visual question answering," in *ICCV*, 2015.
- [138] S. Kazemzadeh, V. Ordonez, M. Matten, and T. Berg, "Referitgame: Referring to objects in photographs of natural scenes," in *EMNLP*, 2014.
- [139] A. Farhadi, M. Hejrati, M. A. Sadeghi, P. Young, C. Rashtchian, J. Hockenmaier, and D. Forsyth, "Every picture tells a story: Generating sentences from images," in *ECCV*, 2010.
- [140] D. Teney, L. Liu, and A. van Den Hengel, "Graph-structured representations for visual question answering," in *CVPR*, 2017.
- [141] M.-C. De Marneffe and C. D. Manning, "The stanford typed dependencies representation," in *Coling 2008: proceedings of the workshop on cross-framework and cross-domain parser evaluation*, 2008.
- [142] K. Cho, B. Van Merriënboer, C. Gulcehre, D. Bahdanau, F. Bougares, H. Schwenk, and Y. Bengio, "Learning phrase representations using rnn encoder-decoder for statistical machine translation," in *EMNLP*, 2014, pp. 1724–1734.
- [143] W. Norcliffe-Brown, S. Vafeias, and S. Parisot, "Learning conditioned graph structures for interpretable visual question answering," *NeurIPS*, vol. 31, 2018.
- [144] R. Hu, A. Rohrbach, T. Darrell, and K. Saenko, "Language-conditioned graph networks for relational reasoning," in *ICCV*, 2019.
- [145] C. Jing, Y. Jia, Y. Wu, X. Liu, and Q. Wu, "Maintaining reasoning consistency in compositional visual question answering," in *CVPR*, 2022.
- [146] L. Li, Z. Gan, Y. Cheng, and J. Liu, "Relation-aware graph attention network for visual question answering," in *ICCV*, 2019.
- [147] E.-S. Kim, W. Y. Kang, K.-W. On, Y.-J. Heo, and B.-T. Zhang, "Hypergraph attention networks for multimodal learning," in *CVPR*, 2020.
- [148] J. Gilmer, S. S. Schoenholz, P. F. Riley, O. Vinyals, and G. E. Dahl, "Neural message passing for quantum chemistry," in *International conference on machine learning*. PMLR, 2017, pp. 1263–1272.
- [149] R. Saqr and K. Narasimhan, "Multimodal graph networks for compositional generalization in visual question answering," *NeurIPS*, vol. 33, 2020.
- [150] K. Xu, W. Hu, J. Leskovec, and S. Jegelka, "How powerful are graph neural networks?" *arXiv preprint arXiv:1810.00826*, 2018.
- [151] Y. Goyal, T. Khot, D. Summers-Stay, D. Batra, and D. Parikh, "Making the v in vqa matter: Elevating the role of image understanding in visual question answering," in *CVPR*, 2017, pp. 6904–6913.
- [152] D. A. Hudson and C. D. Manning, "Gqa: a new dataset for compositional question answering over real-world images," *arXiv preprint arXiv:1902.09506*, vol. 3, 2019.
- [153] D. Gao, K. Li, R. Wang, S. Shan, and X. Chen, "Multi-modal graph neural network for joint reasoning on vision and scene text," in *CVPR*, 2020.
- [154] A. Wu, L. Zhu, Y. Han, and Y. Yang, "Connective cognition network for directional visual commonsense reasoning," *NeurIPS*, vol. 32, 2019.
- [155] W. Yu, J. Zhou, W. Yu, X. Liang, and N. Xiao, "Heterogeneous graph learning for visual commonsense reasoning," *NeurIPS*, vol. 32, 2019.
- [156] D. Teney, P. Anderson, X. He, and A. Van Den Hengel, "Tips and tricks for visual question answering: Learnings from the 2017 challenge," in *CVPR Challenge*, 2018.
- [157] P. Wang, Q. Wu, C. Shen, A. Dick, and A. Van Den Hengel, "Fvqa: Fact-based visual question answering," *IEEE TPAMI*, vol. 40, 2017.
- [158] M. Narasimhan, S. Lazebnik, and A. Schwing, "Out of the box: Reasoning with graph convolution nets for factual visual question answering," *NeurIPS*, vol. 31, 2018.
- [159] A. K. Singh, A. Mishra, S. Shekhar, and A. Chakraborty, "From strings to things: Knowledge-enabled vqa model that can read and reason," in *ICCV*, 2019.
- [160] Y. Li, D. Tarlow, M. Brockschmidt, and R. Zemel, "Gated graph sequence neural networks," *arXiv preprint arXiv:1511.05493*, 2015.
- [161] K. Marino, X. Chen, D. Parikh, A. Gupta, and M. Rohrbach, "Krisp: Integrating implicit and symbolic knowledge for open-domain knowledge-based vqa," in *CVPR*, 2021.
- [162] M. Schlichtkrull, T. N. Kipf, P. Bloem, R. v. d. Berg, I. Titov, and M. Welling, "Modeling relational data with graph convolutional networks," in *ECCV*, 2018.
- [163] J. Park, J. Lee, and K. Sohn, "Bridge to answer: Structure-aware graph interaction network for video question answering," in *CVPR*, 2021.
- [164] W. Yu, H. Zheng, M. Li, L. Ji, L. Wu, N. Xiao, and N. Duan, "Learning from inside: Self-driven siamese sampling and reasoning for video question answering," *NeurIPS*, vol. 34, 2021.
- [165] F. Liu, J. Liu, W. Wang, and H. Lu, "Hair: Hierarchical visual-semantic relational reasoning for video question answering," in *ICCV*, 2021.
- [166] D. Huang, P. Chen, R. Zeng, Q. Du, M. Tan, and C. Gan, "Location-aware graph convolutional networks for video question answering," in *AAAI*, 2020.
- [167] S. Sukhbaatar, J. Weston, R. Fergus *et al.*, "End-to-end memory networks," *NeurIPS*, vol. 28, 2015.
- [168] S. Yang, G. Li, and Y. Yu, "Cross-modal relationship inference for grounding referring expressions," in *CVPR*, 2019.
- [169] —, "Dynamic graph attention for referring expression comprehension," in *ICCV*, 2019.
- [170] —, "Relationship-embedded representation learning for grounding referring expressions," *IEEE TPAMI*, vol. 43, 2020.
- [171] P. Wang, Q. Wu, J. Cao, C. Shen, L. Gao, and A. v. d. Hengel, "Neighbourhood watch: Referring expression comprehension via language-guided graph attention networks," in *CVPR*, 2019.
- [172] S. Chen and B. Li, "Multi-modal dynamic graph transformer for visual grounding," in *CVPR*, 2022.
- [173] S. Huang, T. Hui, S. Liu, G. Li, Y. Wei, J. Han, L. Liu, and B. Li, "Referring image segmentation via cross-modal progressive comprehension," in *CVPR*, 2020.
- [174] T. Hui, S. Liu, S. Huang, G. Li, S. Yu, F. Zhang, and J. Han, "Linguistic structure guided context modeling for referring image segmentation," in *ECCV*, 2020.
- [175] P. Achlioptas, A. Abdelreheem, F. Xia, M. Elhoseiny, and L. Guibas, "Referit3d: Neural listeners for fine-grained 3d object identification in real-world scenes," in *ECCV*, 2020.
- [176] M. Bajaj, L. Wang, and L. Sigal, "G3rground: Graph-based language grounding," in *ICCV*, 2019.
- [177] S. Yang, G. Li, and Y. Yu, "Propagating over phrase relations for one-stage visual grounding," in *ECCV*, 2020.
- [178] Y. Liu, B. Wan, L. Ma, and X. He, "Relation-aware instance refinement for weakly supervised visual grounding," in *CVPR*, 2021.
- [179] Y. Liu, B. Wan, X. Zhu, and X. He, "Learning cross-modal context graph for visual grounding," in *AAAI*, 2020.
- [180] Z. Mu, S. Tang, J. Tan, Q. Yu, and Y. Zhuang, "Disentangled motif-aware graph learning for phrase grounding," in *AAAI*, 2021.
- [181] R. Zellers, M. Yatskar, S. Thomson, and Y. Choi, "Neural motifs: Scene graph parsing with global context," in *CVPR*, 2018.
- [182] Z. Zhang, Z. Zhao, Y. Zhao, Q. Wang, H. Liu, and L. Gao, "Where does it exist: Spatio-temporal video grounding for multi-form sentences," in *CVPR*, 2020.
- [183] Y. Zhao, Z. Zhao, Z. Zhang, and Z. Lin, "Cascaded prediction network via segment tree for temporal video grounding," in *CVPR*, 2021.
- [184] G. Li, C. Xiong, A. Thabet, and B. Ghanem, "Deepergcn: All you need to train deeper gcns," *arXiv preprint arXiv:2006.07739*, 2020.

- [185] J. Li, J. Xie, L. Qian, L. Zhu, S. Tang, F. Wu, Y. Yang, Y. Zhuang, and X. E. Wang, "Compositional temporal grounding with structured variational cross-graph correspondence learning," in *CVPR*, 2022.
- [186] T. Yao, Y. Pan, Y. Li, and T. Mei, "Exploring visual relationship for image captioning," in *ECCV*, 2018, pp. 684–699.
- [187] P. Anderson, X. He, C. Buehler, D. Teney, M. Johnson, S. Gould, and L. Zhang, "Bottom-up and top-down attention for image captioning and visual question answering," in *CVPR*, 2018.
- [188] T. Yao, Y. Pan, Y. Li, and T. Mei, "Hierarchy parsing for image captioning," in *ICCV*, 2019.
- [189] X. Yang, K. Tang, H. Zhang, and J. Cai, "Auto-encoding scene graphs for image captioning," in *CVPR*, 2019.
- [190] Y. Zhong, L. Wang, J. Chen, D. Yu, and Y. Li, "Comprehensive image captioning via scene graph decomposition," in *ECCV*, 2020.
- [191] S. Chen, Q. Jin, P. Wang, and Q. Wu, "Say as you wish: Fine-grained control of image caption generation with abstract scene graphs," in *CVPR*, 2020.
- [192] K. Nguyen, S. Tripathi, B. Du, T. Guha, and T. Q. Nguyen, "In defense of scene graphs for image captioning," in *ICCV*, 2021.
- [193] O. Ulutan, A. Iftekhar, and B. S. Manjunath, "Vsgnet: Spatial attention network for detecting human object interactions using graph convolutions," in *CVPR*, 2020.
- [194] Z. Zhang, Y. Shi, C. Yuan, B. Li, P. Wang, W. Hu, and Z.-J. Zha, "Object relational graph with teacher-recommended learning for video captioning," in *CVPR*, 2020.
- [195] B. Pan, H. Cai, D.-A. Huang, K.-H. Lee, A. Gaidon, E. Adeli, and J. C. Niebles, "Spatio-temporal graph for video captioning with knowledge distillation," in *CVPR*, 2020.
- [196] S. Chen and Y.-G. Jiang, "Motion guided region message passing for video captioning," in *ICCV*, 2021.
- [197] Y. Huang and L. Wang, "Acmm: Aligned cross-modal memory for few-shot image and sentence matching," in *ICCV*, 2019.
- [198] K. Li, Y. Zhang, K. Li, Y. Li, and Y. Fu, "Visual semantic reasoning for image-text matching," in *ICCV*, 2019.
- [199] S. Yan, L. Yu, and Y. Xie, "Discrete-continuous action space policy gradient-based attention for image-text matching," in *CVPR*, 2021.
- [200] H. Wang, Y. Zhang, Z. Ji, Y. Pang, and L. Ma, "Consensus-aware visual-semantic embedding for image-text matching," in *ECCV*, 2020.
- [201] C. Liu, Z. Mao, T. Zhang, H. Xie, B. Wang, and Y. Zhang, "Graph structured network for image-text matching," in *CVPR*, 2020.
- [202] Y. Li, D. Zhang, and Y. Mu, "Visual-semantic matching by exploring high-order attention and distraction," in *CVPR*, 2020.
- [203] S. Chen, Y. Zhao, Q. Jin, and Q. Wu, "Fine-grained video-text retrieval with hierarchical graph reasoning," in *CVPR*, 2020.
- [204] Y. Zeng, D. Cao, X. Wei, M. Liu, Z. Zhao, and Z. Qin, "Multimodal relational graph for cross-modal video moment retrieval," in *CVPR*, 2021.
- [205] J. Li, S. Tang, L. Zhu, H. Shi, X. Huang, F. Wu, Y. Yang, and Y. Zhuang, "Adaptive hierarchical graph reasoning with semantic coherence for video-and-language inference," in *ICCV*, 2021.
- [206] P. Anderson, Q. Wu, D. Teney, J. Bruce, M. Johnson, N. Sünderhauf, I. Reid, S. Gould, and A. Van Den Hengel, "Vision-and-language navigation: Interpreting visually-grounded navigation instructions in real environments," in *CVPR*, 2018.
- [207] Z. Deng, K. Narasimhan, and O. Russakovsky, "Evolving graphical planner: Contextual global planning for vision-and-language navigation," *NeurIPS*, vol. 33, 2020.
- [208] K. Chen, J. K. Chen, J. Chuang, M. Vázquez, and S. Savarese, "Topological planning with transformers for vision-and-language navigation," in *CVPR*, 2021.
- [209] C. Gao, J. Chen, S. Liu, L. Wang, Q. Zhang, and Q. Wu, "Room-and-object aware knowledge reasoning for remote embodied referring expression," in *CVPR*, 2021.
- [210] J. Chen, C. Gao, E. Meng, Q. Zhang, and S. Liu, "Reinforced structured state-evolution for vision-language navigation," in *CVPR*, 2022.
- [211] S. Chen, P.-L. Guhur, M. Tapaswi, C. Schmid, and I. Laptev, "Think global, act local: Dual-scale graph transformer for vision-and-language navigation," in *CVPR*, 2022.
- [212] C. R. Qi, H. Su, K. Mo, and L. J. Guibas, "Pointnet: Deep learning on point sets for 3d classification and segmentation," in *CVPR*, 2017.
- [213] H. Thomas, C. R. Qi, J.-E. Deschaud, B. Marcotegui, F. Goulette, and L. J. Guibas, "Kpconv: Flexible and deformable convolution for point clouds," in *ICCV*, 2019.
- [214] Y. Li, R. Bu, M. Sun, W. Wu, X. Di, and B. Chen, "Pointcnn: Convolution on x-transformed points," *NeurIPS*, vol. 31, 2018.
- [215] W. Wu, Z. Qi, and L. Fuxin, "Pointconv: Deep convolutional networks on 3d point clouds," in *CVPR*, 2019, pp. 9621–9630.
- [216] C. R. Qi, L. Yi, H. Su, and L. J. Guibas, "Pointnet++: Deep hierarchical feature learning on point sets in a metric space," *NeurIPS*, vol. 30, 2017.
- [217] M. Simonovsky and N. Komodakis, "Dynamic edge-conditioned filters in convolutional neural networks on graphs," in *CVPR*, 2017.
- [218] K. Zhang, M. Hao, J. Wang, X. Chen, Y. Leng, C. W. de Silva, and C. Fu, "Linked dynamic graph cnn: Learning through point cloud by linking hierarchical features," in *M2VIP*, 2021.
- [219] K. Hassani and M. Haley, "Unsupervised multi-task feature learning on point clouds," in *ICCV*, 2019.
- [220] Z.-H. Lin, S.-Y. Huang, and Y.-C. F. Wang, "Convolution in the cloud: Learning deformable kernels in 3d graph convolution networks for point cloud analysis," in *CVPR*, 2020.
- [221] H. Zhou, Y. Feng, M. Fang, M. Wei, J. Qin, and T. Lu, "Adaptive graph convolution for point cloud analysis," in *ICCV*, 2021.
- [222] Y. Shen, C. Feng, Y. Yang, and D. Tian, "Mining point cloud local structures by kernel correlation and graph pooling," in *CVPR*, 2018.
- [223] C. Chen, G. Li, R. Xu, T. Chen, M. Wang, and L. Lin, "Cluster-net: Deep hierarchical cluster network with rigorously rotation-invariant representation for point cloud analysis," in *CVPR*, 2019.
- [224] T. Xiang, C. Zhang, Y. Song, J. Yu, and W. Cai, "Walk in the cloud: Learning curves for point clouds shape analysis," in *ICCV*, 2021.
- [225] M. Lin and A. Feragen, "diffconv: Analyzing irregular point clouds with an irregular view," in *ECCV*, 2022.
- [226] R. Wiersma, A. Nasikun, E. Eisemann, and K. Hildebrandt, "Deltaconv: Anisotropic operators for geometric deep learning on point clouds," *ACM TOG*, 2022.
- [227] C. Wang, B. Samari, and K. Siddiqi, "Local spectral graph convolution for point set feature learning," in *ECCV*, 2018.
- [228] Y. Feng, H. You, Z. Zhang, R. Ji, and Y. Gao, "Hypergraph neural networks," in *AAAI*, vol. 33, 2019.
- [229] L. Yi, H. Su, X. Guo, and L. J. Guibas, "Syncspecnn: Synchronized spectral cnn for 3d shape segmentation," in *CVPR*, 2017.
- [230] G. Te, W. Hu, A. Zheng, and Z. Guo, "Rgcn: Regularized graph cnn for point cloud segmentation," in *ACM MM*, 2018.
- [231] G. Pan, J. Wang, R. Ying, and P. Liu, "3dti-net: Learn inner transform invariant 3d geometry features using dynamic gcn," *arXiv preprint arXiv:1812.06254*, 2018.
- [232] Y. Zhang and M. Rabbat, "A graph-cnn for 3d point cloud classification," in *ICASSP*, 2018.
- [233] C. Chen, L. Z. Fragonara, and A. Tsourdos, "Gapnet: Graph attention based point neural network for exploiting local feature of point cloud," *CoRR*, vol. abs/1905.08705, 2019.
- [234] L. Wang, Y. Huang, Y. Hou, S. Zhang, and J. Shan, "Graph attention convolution for point cloud semantic segmentation," in *CVPR*, 2019.
- [235] L. Xun, X. Feng, C. Chen, X. Yuan, and Q. Lu, "Graph attention-based deep neural network for 3d point cloud processing," in *ICME*. IEEE, 2021.
- [236] C.-Q. Huang, F. Jiang, Q.-H. Huang, X.-Z. Wang, Z.-M. Han, and W.-Y. Huang, "Dual-graph attention convolution network for 3-d point cloud classification," *IEEE Transactions on Neural Networks and Learning Systems*, 2022.
- [237] P. Gomes, S. Rossi, and L. Toni, "Spatio-temporal graph-rnn for point cloud prediction," in *ICIP*. IEEE, 2021.
- [238] D. Lu, Q. Xie, K. Gao, L. Xu, and J. Li, "3dctn: 3d convolution-transformer network for point cloud classification," *IEEE TITS*, 2022.
- [239] J. Liu, B. Ni, C. Li, J. Yang, and Q. Tian, "Dynamic points agglomeration for hierarchical point sets learning," in *ICCV*, 2019.
- [240] Q. Xu, X. Sun, C.-Y. Wu, P. Wang, and U. Neumann, "Grid-gcn for fast and scalable point cloud learning," in *CVPR*, 2020.
- [241] H. Lei, N. Akhtar, and A. Mian, "Spherical kernel for efficient graph convolution on 3d point clouds," *IEEE TPAMI*, vol. 43, 2020.
- [242] J.-F. Zhang and Z. Zhang, "Point-x: A spatial-locality-aware architecture for energy-efficient graph-based point-cloud deep learning," in *IEEE/ACM International Symposium on Microarchitecture*, 2021.
- [243] Y. Li, H. Chen, Z. Cui, R. Timofte, M. Pollefeys, G. Chirikjian, and L. Van Gool, "Towards efficient graph convolutional networks for point cloud handling," in *ICCV*, 2021.

- [244] T. Le and Y. Duan, "Pointgrid: A deep network for 3d shape understanding," in *CVPR*, 2018.
- [245] Y. Xu, T. Fan, M. Xu, L. Zeng, and Y. Qiao, "Spidernn: Deep learning on point sets with parameterized convolutional filters," in *ECCV*, 2018.
- [246] Y. Wang, Y. Sun, Z. Liu, S. E. Sarma, M. M. Bronstein, and J. M. Solomon, "Dynamic graph cnn for learning on point clouds," *ACM Trans. Graph.*, 2019.
- [247] R. Hanocka, A. Hertz, N. Fish, R. Giryas, S. Fleishman, and D. Cohen-Or, "Meshcnn: a network with an edge," *ACM TOG*, vol. 38, 2019.
- [248] Y. Feng, Y. Feng, H. You, X. Zhao, and Y. Gao, "Meshnet: Mesh neural network for 3d shape representation," in *AAAI*, 2019.
- [249] C. Lian, L. Wang, T. H. Wu, M. Liu, F. Durán, C. C. Ko, and D. Shen, "Meshsnet: Deep multi-scale mesh feature learning for end-to-end tooth labeling on 3d dental surfaces," in *MICCAI*, 2019, pp. 837–845.
- [250] N. Verma, E. Boyer, and J. Verbeek, "Feastnet: Feature-steered graph convolutions for 3d shape analysis," in *CVPR*, 2018.
- [251] S. Gong, L. Chen, M. Bronstein, and S. Zafeiriou, "Spiralnet++: A fast and highly efficient mesh convolution operator," in *ICCV Workshops*, 2019.
- [252] F. Milano, A. Loquercio, A. Rosinol, D. Scaramuzza, and L. Carlone, "Primal-dual mesh convolutional neural networks," *NeurIPS*, vol. 33, 2020.
- [253] V. V. Singh, S. V. Sheshappanavar, and C. Kambhamettu, "Mesh classification with dilated mesh convolutions," in *ICIP*. IEEE, 2021.
- [254] M. Yavartanoo, S.-H. Hung, R. Neshatavar, Y. Zhang, and K. M. Lee, "Polynet: Polynomial neural network for 3d shape recognition with polyshape representation," in *3DV*. IEEE, 2021.
- [255] W. He, Z. Jiang, C. Zhang, and A. M. Sainju, "Curvanet: Geometric deep learning based on directional curvature for 3d shape analysis," in *KDD*, 2020.
- [256] L. He, Y. Dong, Y. Wang, D. Tao, and Z. Lin, "Gauge equivariant transformer," in *NeurIPS*, 2021.
- [257] S.-M. Hu, Z.-N. Liu, M.-H. Guo, J.-X. Cai, J. Huang, T.-J. Mu, and R. R. Martin, "Subdivision-based mesh convolution networks," *TOG*, vol. 41, 2022.
- [258] Q. Dong, Z. Wang, J. Gao, S. Chen, Z. Shu, and S. Xin, "Laplacian2mesh: Laplacian-based mesh understanding," *arXiv preprint arXiv:2202.00307*, 2022.
- [259] A. Lahav and A. Tal, "Meshwalker: Deep mesh understanding by random walks," *TOG*, vol. 39, 2020.
- [260] J. Schult, F. Engelmann, T. Kontogianni, and B. Leibe, "Dualconvmesh-net: Joint geodesic and euclidean convolutions on 3d meshes," in *CVPR*, 2020.
- [261] G. Bouritsas, S. Bokhnyak, S. Ploumpis, M. Bronstein, and S. Zafeiriou, "Neural 3d morphable models: Spiral convolutional networks for 3d shape representation learning and generation," in *ICCV*, 2019.
- [262] R. B. Izhak, A. Lahav, and A. Tal, "Attwalk: Attentive cross-walks for deep mesh analysis," in *WACV*, 2022.
- [263] J. Wang, Q. Xie, Y. Xu, L. Zhou, and N. Ye, "Cluttered indoor scene modeling via functional part-guided graph matching," *Comput. Aided Geom. Des.*, 2016.
- [264] X. Qi, R. Liao, J. Jia, S. Fidler, and R. Urtasun, "3d graph neural networks for rgb-d semantic segmentation," in *ICCV*, 2017.
- [265] L. Loic and S. Martin, "Large-scale point cloud semantic segmentation with superpoint graphs," in *CVPR*, 2018.
- [266] L. Loic and B. Mohamed, "Point cloud oversegmentation with graph-structured deep metric learning," in *CVPR*, 2019.
- [267] L. Wang, Y. Huang, Y. Hou, S. Zhang, and J. Shan, "Graph attention convolution for point cloud semantic segmentation," in *CVPR*, 2019.
- [268] K. Zhiheng and L. Ning, "Pyramnet: Point cloud pyramid attention network and graph embedding module for classification and segmentation," *arXiv preprint arXiv:1906.03299*, 2019.
- [269] L. Jiang, H. Zhao, S. Liu, X. Shen, C.-W. Fu, and J. Jia, "Hierarchical point-edge interaction network for point cloud semantic segmentation," in *ICCV*, 2019.
- [270] H. Zhao, L. Jiang, C.-W. Fu, and J. Jia, "PointWeb: Enhancing local neighborhood features for point cloud processing," in *CVPR*, 2019.
- [271] Z. Liang, M. Yang, L. Deng, C. Wang, and B. Wang, "Hierarchical depthwise graph convolutional neural network for 3d semantic segmentation of point clouds," in *ICRA*. IEEE, 2019.
- [272] H. Lei, N. Akhtar, and A. Mian, "Seggcn: Efficient 3d point cloud segmentation with fuzzy spherical kernel," in *CVPR*, 2020.
- [273] Y. Ma, Y. Guo, H. Liu, Y. Lei, and G. Wen, "Global context reasoning for semantic segmentation of 3d point clouds," in *WACV*, 2020.
- [274] Q. Xu, X. Sun, C.-Y. Wu, P. Wang, and U. Neumann, "Grid-gcn for fast and scalable point cloud learning," in *CVPR*, 2020.
- [275] Q. Hu, B. Yang, L. Xie, S. Rosa, Y. Guo, Z. Wang, N. Trigoni, and A. Markham, "Randla-net: Efficient semantic segmentation of large-scale point clouds," in *CVPR*, 2020.
- [276] W. Han, C. Wen, C. Wang, X. Li, and Q. Li, "Point2node: Correlation learning of dynamic-node for point cloud feature modeling," in *AAAI*, 2020.
- [277] M. Xu, R. Ding, H. Zhao, and X. Qi, "Paconv: Position adaptive convolution with dynamic kernel assembling on point clouds," in *CVPR*, 2021.
- [278] A. Tao, Y. Duan, Y. Wei, J. Lu, and J. Zhou, "SegGroup: Seg-level supervision for 3D instance and semantic segmentation," *IEEE TIP*, 2022.
- [279] M. Tatarchenko, J. Park, V. Koltun, and Q.-Y. Zhou, "Tangent convolutions for dense prediction in 3d," in *CVPR*, 2018.
- [280] C. Choy, J. Gwak, and S. Savarese, "4d spatio-temporal convnets: Minkowski convolutional neural networks," in *CVPR*, 2019.
- [281] S. Wang, S. Suo, W. Ma, A. Pokrovsky, and R. Urtasun, "Deep parametric continuous convolutional neural networks," in *CVPR*, 2018.
- [282] Y. Wang and J. M. Solomon, "Object dgcnn: 3d object detection using dynamic graphs," *NeurIPS*, vol. 34, 2021.
- [283] M. Liang, B. Yang, S. Wang, and R. Urtasun, "Deep continuous fusion for multi-sensor 3d object detection," in *ECCV*, 2018.
- [284] S. Lan, R. Yu, G. Yu, and L. S. Davis, "Modeling local geometric structure of 3d point clouds using geo-cnn," in *CVPR*, 2019.
- [285] J. Zarzar, S. Giancola, and B. Ghanem, "Pointrgcn: Graph convolution networks for 3d vehicles detection refinement," *arXiv preprint arxiv:1911.12236*, 2019.
- [286] J. Chen, B. Lei, Q. Song, H. Ying, D. Z. Chen, and J. Wu, "A hierarchical graph network for 3d object detection on point clouds," in *CVPR*, 2020.
- [287] W. Shi and R. R. Rajkumar, "Point-gnn: Graph neural network for 3d object detection in a point cloud," in *CVPR*, 2020.
- [288] M. Feng, S. Z. Gilani, Y. Wang, L. Zhang, and A. Mian, "Relation graph network for 3d object detection in point clouds," *TIP*, vol. 30, 2020.
- [289] P.-H. Huang, H.-H. Lee, H.-T. Chen, and T.-L. Liu, "Text-guided graph neural networks for referring 3d instance segmentation," in *AAAI*, 2021.
- [290] Z. Yuan, X. Yan, Y. Liao, R. Zhang, S. Wang, Z. Li, and S. Cui, "Instancerefer: Cooperative holistic understanding for visual grounding on point clouds through instance multi-level contextual referring," in *ICCV*, 2021.
- [291] M. Feng, Z. Li, Q. Li, L. Zhang, X. Zhang, G. Zhu, H. Zhang, Y. Wang, and A. Mian, "Free-form description guided 3d visual graph network for object grounding in point cloud," in *ICCV*, 2021.
- [292] L. Pan, "Ecg: Edge-aware point cloud completion with graph convolution," *IEEE RA-L*, vol. 5, 2020.
- [293] L. Zhu, B. Wang, G. Tian, W. Wang, and C. Li, "Towards point cloud completion: Point rank sampling and cross-cascade graph cnn," *Neurocomputing*, vol. 461, 2021.
- [294] J. Shi, L. Xu, L. Heng, and S. Shen, "Graph-guided deformation for point cloud completion," *IEEE RA-L*, vol. 6, 2021.
- [295] W. Yifan, S. Wu, H. Huang, D. Cohen-Or, and O. Sorkine-Hornung, "Patch-based progressive 3d point set upsampling," in *CVPR*, 2019.
- [296] G. Qian, A. Abualshour, G. Li, A. Thabet, and B. Ghanem, "Pu-gcn: Point cloud upsampling using graph convolutional networks," in *CVPR*, 2021.
- [297] H. Wu, J. Zhang, and K. Huang, "Point cloud super resolution with adversarial residual graph networks," *arXiv preprint arXiv:1908.02111*, 2019.
- [298] Y. Qian, J. Hou, S. Kwong, and Y. He, "Pugeo-net: A geometry-centric network for 3d point cloud upsampling," in *ECCV*, 2020.
- [299] F. Pistilli, G. Fracastoro, D. Valsesia, and E. Magli, "Learning graph-convolutional representations for point cloud denoising," in *ECCV*, 2020.
- [300] S. Luo and W. Hu, "Differentiable manifold reconstruction for point cloud denoising," in *ACM MM*, 2020.

- [301] M. Armando, J.-S. Franco, and E. Boyer, "Mesh denoising with facet graph convolutions," *IEEE TVCG*, 2020.
- [302] Y. Shen, H. Fu, Z. Du, X. Chen, E. Burnaev, D. Zorin, K. Zhou, and Y. Zheng, "Gcn-denoiser: Mesh denoising with graph convolutional networks," *ACM TOG*, vol. 41, 2022.
- [303] Y. Zhang, G. Shen, Q. Wang, Y. Qian, M. Wei, and J. Qin, "Geobi-gnn: Geometry-aware bi-domain mesh denoising via graph neural networks," *Computer-Aided Design*, vol. 144, 2022.
- [304] Y. Yang, C. Feng, Y. Shen, and D. Tian, "Foldingnet: Point cloud auto-encoder via deep grid deformation," in *CVPR*, 2018.
- [305] K. Mo, P. Guerrero, L. Yi, H. Su, P. Wonka, N. J. Mitra, and L. J. Guibas, "StructureNet: hierarchical graph networks for 3d shape generation," *ACM TOG*, vol. 38, 2019.
- [306] D. Valsesia, G. Fracastoro, and E. Magli, "Learning localized generative models for 3d point clouds via graph convolution," in *ICLR*, 2018.
- [307] D. W. Shu, S. W. Park, and J. Kwon, "3d point cloud generative adversarial network based on tree structured graph convolutions," in *ICCV*, 2019.
- [308] Y. Li and G. Baciú, "Hsgan: Hierarchical graph learning for point cloud generation," *IEEE TIP*, vol. 30, 2021.
- [309] N. Wang, Y. Zhang, Z. Li, Y. Fu, W. Liu, and Y.-G. Jiang, "Pixel2mesh: Generating 3d mesh models from single rgb images," in *ECCV*, 2018.
- [310] C. Wen, Y. Zhang, Z. Li, and Y. Fu, "Pixel2mesh++: Multi-view 3d mesh generation via deformation," in *ICCV*, 2019.
- [311] G. Gkioxari, J. Malik, and J. Johnson, "Mesh r-cnn," in *ICCV*, 2019, pp. 9785–9795.
- [312] K. He, G. Gkioxari, P. Dollár, and R. Girshick, "Mask r-cnn," in *ICCV*, 2017.
- [313] U. Wickramasinghe, E. Remelli, G. Knott, and P. Fua, "Voxel2mesh: 3d mesh model generation from volumetric data," in *MICCAI*, 2020.
- [314] H. Dhama, F. Manhardt, N. Navab, and F. Tombari, "Graph-to-3d: End-to-end generation and manipulation of 3d scenes using scene graphs," in *ICCV*, 2021.
- [315] N. Kolotouros, G. Pavlakos, and K. Daniilidis, "Convolutional mesh regression for single-image human shape reconstruction," in *CVPR*, 2019.
- [316] X. Yu, J. van Baar, and S. Chen, "Joint 3d human shape recovery and pose estimation from a single image with bilayer graph," in *3DV*, 2021.
- [317] S. Zhou, M. Jiang, S. Cai, and Y. Lei, "Dc-gnet: Deep mesh relation capturing graph convolution network for 3d human shape reconstruction," in *ACM MM*, 2021.
- [318] H. Choi, G. Moon, and K. M. Lee, "Pose2mesh: Graph convolutional network for 3d human pose and mesh recovery from a 2d human pose," in *ECCV*, 2020.
- [319] C. Zheng, M. Mendieta, P. Wang, A. Lu, and C. Chen, "A lightweight graph transformer network for human mesh reconstruction from 2d human pose," *arXiv preprint arXiv:2111.12696*, 2021.
- [320] J. Lin, Y. Yuan, T. Shao, and K. Zhou, "Towards high-fidelity 3d face reconstruction from in-the-wild images using graph convolutional networks," in *CVPR*, 2020.
- [321] S. Cheng, G. Tzimiropoulos, J. Shen, and M. Pantic, "Faster, better and more detailed: 3d face reconstruction with graph convolutional networks," in *ACCV*, 2020.
- [322] L. Ge, Z. Ren, Y. Li, Z. Xue, Y. Wang, J. Cai, and J. Yuan, "3d hand shape and pose estimation from a single rgb image," in *CVPR*, 2019.
- [323] M. Li, L. An, H. Zhang, L. Wu, F. Chen, T. Yu, and Y. Liu, "Interacting attention graph for single image two-hand reconstruction," in *CVPR*, 2022.
- [324] A. S. Heinsfeld, A. R. Franco, R. C. Craddock, A. Buchweitz, and F. Meneguzzi, "Identification of autism spectrum disorder using deep learning and the abide dataset," *NeuroImage: Clinical*, vol. 17, 2018.
- [325] S. Parisot, S. I. Ktena, E. Ferrante, M. Lee, R. G. Moreno, B. Glocker, and D. Rueckert, "Spectral graph convolutions for population-based disease prediction," in *MICCAI*, 2017.
- [326] R. Anirudh and J. J. Thiagarajan, "Bootstrapping graph convolutional neural networks for autism spectrum disorder classification," in *ICASSP*, 2019.
- [327] Z. Rakhimberdina and T. Murata, "Linear graph convolutional model for diagnosing brain disorders," in *International Conference on Complex Networks and Their Applications*, 2019.
- [328] H. Jiang, P. Cao, M. Xu, J. Yang, and O. Zaiane, "Hi-gcn: a hierarchical graph convolution network for graph embedding learning of brain network and brain disorders prediction," *Computers in Biology and Medicine*, vol. 127, 2020.
- [329] L. Peng, N. Wang, N. Dvornek, X. Zhu, and X. Li, "FedNI: Federated graph learning with network inpainting for population-based disease prediction," *IEEE TMI*, 2022.
- [330] S. I. Ktena, S. Parisot, E. Ferrante, M. Rajchl, M. Lee, B. Glocker, and D. Rueckert, "Distance metric learning using graph convolutional networks: Application to functional brain networks," in *MICCAI*, 2017.
- [331] D. Yao, M. Liu, M. Wang, C. Lian, J. Wei, L. Sun, J. Sui, and D. Shen, "Triplet graph convolutional network for multi-scale analysis of functional connectivity using functional mri," in *International Workshop on Graph Learning in Medical Imaging*. Springer, 2019, pp. 70–78.
- [332] X. Li, Y. Zhou, N. C. Dvornek, M. Zhang, J. Zhuang, P. Ventola, and J. S. Duncan, "Pooling regularized graph neural network for fmri biomarker analysis," in *MICCAI*, 2020.
- [333] X. Li, Y. Zhou, N. Dvornek, M. Zhang, S. Gao, J. Zhuang, D. Scheinost, L. H. Staib, P. Ventola, and J. S. Duncan, "BrainGNN: Interpretable brain graph neural network for fmri analysis," *MedIA*, vol. 74, 2021.
- [334] A. Kazi, S. Shekarforoush, S. Arvind Krishna, H. Burwinkel, G. Vivar, K. Kortüm, S.-A. Ahmadi, S. Albarqouni, and N. Navab, "Inceptiongcn: receptive field aware graph convolutional network for disease prediction," in *IPMI*, 2019.
- [335] D. Yao, J. Sui, E. Yang, P.-T. Yap, D. Shen, and M. Liu, "Temporal-adaptive graph convolutional network for automated identification of major depressive disorder using resting-state fmri," in *International Workshop on Machine Learning in Medical Imaging*. Springer, 2020, pp. 1–10.
- [336] D. Yao, E. Yang, H. Guan, J. Sui, Z. Zhang, and M. Liu, "Tensor-based multi-index representation learning for major depression disorder detection with resting-state fmri," in *MICCAI*, 2021.
- [337] H. Yang, X. Li, Y. Wu, S. Li, S. Lu, J. S. Duncan, J. C. Gee, and S. Gu, "Interpretable multimodality embedding of cerebral cortex using attention graph network for identifying bipolar disorder," in *MICCAI*, 2019.
- [338] Y. Zhang, L. Tetrel, B. Thirion, and P. Bellec, "Functional annotation of human cognitive states using deep graph convolution," *NeuroImage*, vol. 231, 2021.
- [339] S. Gadgil, Q. Zhao, A. Pfefferbaum, E. V. Sullivan, E. Adeli, and K. M. Pohl, "Spatio-temporal graph convolution for resting-state fmri analysis," in *MICCAI*, 2020.
- [340] B.-H. Kim, J. C. Ye, and J.-J. Kim, "Learning dynamic graph representation of brain connectome with spatio-temporal attention," *NeurIPS*, vol. 34, 2021.
- [341] S. Parisot, S. I. Ktena, E. Ferrante, M. Lee, R. Guerrero, B. Glocker, and D. Rueckert, "Disease prediction using graph convolutional networks: application to autism spectrum disorder and alzheimer's disease," *MedIA*, vol. 48, 2018.
- [342] X. Zhao, F. Zhou, L. Ou-Yang, T. Wang, and B. Lei, "Graph convolutional network analysis for mild cognitive impairment prediction," in *ISBI*, 2019.
- [343] J. Liu, G. Tan, W. Lan, and J. Wang, "Identification of early mild cognitive impairment using multi-modal data and graph convolutional networks," *BMC bioinformatics*, vol. 21, 2020.
- [344] S. Yu, S. Wang, X. Xiao, J. Cao, G. Yue, D. Liu, T. Wang, Y. Xu, and B. Lei, "Multi-scale enhanced graph convolutional network for early mild cognitive impairment detection," in *MICCAI*, 2020.
- [345] Y. Huang and A. Chung, "Edge-variational graph convolutional networks for uncertainty-aware disease prediction," in *MICCAI*, 2020.
- [346] K. Gopinath, C. Desrosiers, and H. Lombaert, "Learnable pooling in graph convolution networks for brain surface analysis," *IEEE TPAMI*, 2020.
- [347] J. Ma, X. Zhu, D. Yang, J. Chen, and G. Wu, "Attention-guided deep graph neural network for longitudinal alzheimer's disease analysis," in *MICCAI*, 2020.
- [348] C.-Y. Wee, C. Liu, A. Lee, J. S. Poh, H. Ji, A. Qiu, A. D. N. Initiative et al., "Cortical graph neural network for ad and mci diagnosis and transfer learning across populations," *NeuroImage: Clinical*, vol. 23, 2019.
- [349] X. Zhang, L. He, K. Chen, Y. Luo, J. Zhou, and F. Wang, "Multi-view graph convolutional network and its applications



- on neuroimage analysis for parkinson's disease," in *AMIA Annual Symposium Proceedings*, 2018.
- [350] A. Kazi, S. Shekarforoush, S. Arvind Krishna, H. Burwinkel, G. Vivar, B. Wiestler, K. Kortüm, S.-A. Ahmadi, S. Albarqouni, and N. Navab, "Graph convolution based attention model for personalizable disease prediction," in *MICCAI*, 2019.
- [351] W. Zhang, L. Zhan, P. Thompson, and Y. Wang, "Deep representation learning for multimodal brain networks," in *MICCAI*, 2020.
- [352] X. Yu, S. Lu, L. Guo, S.-H. Wang, and Y.-D. Zhang, "Resgnet-c: A graph convolutional neural network for detection of covid-19," *Neurocomputing*, vol. 452, 2021.
- [353] S.-H. Wang, V. V. Govindaraj, J. M. Górriz, X. Zhang, and Y.-D. Zhang, "Covid-19 classification by fgcn with deep feature fusion from graph convolutional network and convolutional neural network," *Information Fusion*, vol. 67, 2021.
- [354] Y. Zhang, X. Wang, Z. Xu, Q. Yu, A. Yuille, and D. Xu, "When radiology report generation meets knowledge graph," in *AAAI*, 2020.
- [355] D. Hou, Z. Zhao, and S. Hu, "Multi-label learning with visual-semantic embedded knowledge graph for diagnosis of radiology imaging," *IEEE Access*, vol. 9, 2021.
- [356] Y. Liu, F. Zhang, Q. Zhang, S. Wang, Y. Wang, and Y. Yu, "Cross-view correspondence reasoning based on bipartite graph convolutional network for mammogram mass detection," in *CVPR*, 2020.
- [357] Y. Liu, F. Zhang, C. Chen, S. Wang, Y. Wang, and Y. Yu, "Act like a radiologist: Towards reliable multi-view correspondence reasoning for mammogram mass detection," *IEEE TPAMI*, 2021.
- [358] J. Lian, J. Liu, S. Zhang, K. Gao, X. Liu, D. Zhang, and Y. Yu, "A structure-aware relation network for thoracic diseases detection and segmentation," *IEEE TMI*, vol. 40, 2021.
- [359] Z. Chen, J. Liu, M. Zhu, P. Y. Woo, and Y. Yuan, "Instance importance-aware graph convolutional network for 3d medical diagnosis," *MedIA*, vol. 78, 2022.
- [360] P. Gong, Z. Yin, Y. Wang, and Y. Yu, "Towards robust bone age assessment: rethinking label noise and ambiguity," in *MICCAI*, 2020.
- [361] G. Zhao, Q. Feng, C. Chen, Z. Zhou, and Y. Yu, "Diagnose like a radiologist: Hybrid neuro-probabilistic reasoning for attribute-based medical image diagnosis," *IEEE TPAMI*, 2021.
- [362] G. Cucurull, K. Wagstyl, A. Casanova, P. Veličković, E. Jakobsen, M. Drozdal, A. Romero, A. Evans, and Y. Bengio, "Convolutional neural networks for mesh-based parcellation of the cerebral cortex," in *MIDL*, 2018.
- [363] K. Gopinath, C. Desrosiers, and H. Lombaert, "Adaptive graph convolution pooling for brain surface analysis," in *IPMI*, 2019.
- [364] Z. Wu, F. Zhao, J. Xia, L. Wang, W. Lin, J. H. Gilmore, G. Li, and D. Shen, "Intrinsic patch-based cortical anatomical parcellation using graph convolutional neural network on surface manifold," in *MICCAI*, 2019.
- [365] R. He, K. Gopinath, C. Desrosiers, and H. Lombaert, "Spectral graph transformer networks for brain surface parcellation," in *ISBI*, 2020.
- [366] J. M. Wolterink, T. Leiner, and I. Išgum, "Graph convolutional networks for coronary artery segmentation in cardiac ct angiography," in *International Workshop on Graph Learning in Medical Imaging*, 2019.
- [367] Z. Zhai, M. Staring, X. Zhou, Q. Xie, X. Xiao, M. Els Bakker, L. J. Kroft, B. P. Lelieveldt, G. J. Boon, F. A. Klok *et al.*, "Linking convolutional neural networks with graph convolutional networks: application in pulmonary artery-vein separation," in *International Workshop on Graph Learning in Medical Imaging*, 2019.
- [368] S. Y. Shin, S. Lee, I. D. Yun, and K. M. Lee, "Deep vessel segmentation by learning graphical connectivity," *MedIA*, vol. 58, 2019.
- [369] K. J. Noh, S. J. Park, and S. Lee, "Combining fundus images and fluorescein angiography for artery/vein classification using the hierarchical vessel graph network," in *MICCAI*, 2020.
- [370] L. Chen, T. Hatsukami, J.-N. Hwang, and C. Yuan, "Automated intracranial artery labeling using a graph neural network and hierarchical refinement," in *MICCAI*, 2020.
- [371] L. Yao, P. Jiang, Z. Xue, Y. Zhan, D. Wu, L. Zhang, Q. Wang, F. Shi, and D. Shen, "Graph convolutional network based point cloud for head and neck vessel labeling," in *International Workshop on Machine Learning in Medical Imaging*, 2020.
- [372] H. Yang, X. Zhen, Y. Chi, L. Zhang, and X.-S. Hua, "Cpr-gcn: Conditional partial-residual graph convolutional network in automated anatomical labeling of coronary arteries," in *CVPR*, 2020.
- [373] X. Zhang, Z. Cui, J. Feng, Y. Song, D. Wu, and D. Shen, "Corlab-net: Anatomical dependency-aware point-cloud learning for automatic labeling of coronary arteries," in *MLMI*, 2021.
- [374] G. Zhao, K. Liang, C. Pan, F. Zhang, X. Wu, X. Hu, and Y. Yu, "Graph convolution based cross-network multi-scale feature fusion for deep vessel segmentation," *IEEE TMI*, 2022.
- [375] R. Selvan, T. Kipf, M. Welling, J. H. Pedersen, J. Petersen, and M. de Bruijne, "Extraction of airways using graph neural networks," in *MIDL*, 2018.
- [376] A. Garcia-Uceda Juarez, R. Selvan, Z. Saghir, and M. d. Bruijne, "A joint 3d unet-graph neural network-based method for airway segmentation from chest cts," in *MLMI*, 2019.
- [377] O. Ronneberger, P. Fischer, and T. Brox, "U-net: Convolutional networks for biomedical image segmentation," in *MICCAI*, 2015.
- [378] R. Selvan, T. Kipf, M. Welling, A. G.-U. Juarez, J. H. Pedersen, J. Petersen, and M. de Bruijne, "Graph refinement based airway extraction using mean-field networks and graph neural networks," *MedIA*, vol. 64, 2020.
- [379] R. D. S. Mukul, N. Navab, S. Albarqouni *et al.*, "An uncertainty-driven gcn refinement strategy for organ segmentation," *Machine Learning for Biomedical Imaging*, vol. 1, 2020.
- [380] Z. Tian, X. Li, Y. Zheng, Z. Chen, Z. Shi, L. Liu, and B. Fei, "Graph-convolutional-network-based interactive prostate segmentation in mr images," *Medical physics*, vol. 47, 2020.
- [381] Y. Meng, M. Wei, D. Gao, Y. Zhao, X. Yang, X. Huang, and Y. Zheng, "Cnn-gcn aggregation enabled boundary regression for biomedical image segmentation," in *MICCAI*, 2020.
- [382] Y. Meng, W. Meng, D. Gao, Y. Zhao, X. Yang, X. Huang, and Y. Zheng, "Regression of instance boundary by aggregated cnn and gcn," in *ECCV*, 2020.
- [383] C.-H. Chao, Z. Zhu, D. Guo, K. Yan, T.-Y. Ho, J. Cai, A. P. Harrison, X. Ye, J. Xiao, A. Yuille *et al.*, "Lymph node gross tumor volume detection in oncology imaging via relationship learning using graph neural network," in *MICCAI*, 2020.
- [384] Z. Yan, K. Youyong, W. Jiasong, G. Coatrieux, and S. Huazhong, "Brain tissue segmentation based on graph convolutional networks," in *ICIP*, 2019.
- [385] L. Chen, P. Bentley, K. Mori, K. Misawa, M. Fujiwara, and D. Rueckert, "Self-supervised learning for medical image analysis using image context restoration," *MedIA*, vol. 58, 2019.
- [386] H.-Y. Zhou, S. Yu, C. Bian, Y. Hu, K. Ma, and Y. Zheng, "Comparing to learn: Surpassing imagenet pretraining on radiographs by comparing image representations," in *MICCAI*, 2020.
- [387] Z. Zhou, V. Sodha, J. Pang, M. B. Gotway, and J. Liang, "Models genesis," *MedIA*, vol. 67, 2021.
- [388] H.-Y. Zhou, C. Lu, S. Yang, X. Han, and Y. Yu, "Preservational learning improves self-supervised medical image models by reconstructing diverse contexts," in *ICCV*, 2021.
- [389] M. Gutmann and A. Hyvärinen, "Noise-contrastive estimation: A new estimation principle for unnormalized statistical models," in *AISTATS*, 2010.
- [390] L. Ehrlinger and W. Wöß, "Towards a definition of knowledge graphs." *SEMANTiCS (Posters, Demos, SuCCESS)*, vol. 48, 2016.
- [391] Q. Wang, Z. Mao, B. Wang, and L. Guo, "Knowledge graph embedding: A survey of approaches and applications," *IEEE TKDE*, vol. 29, 2017.
- [392] Y. Zhang, H. Jiang, Y. Miura, C. D. Manning, and C. P. Langlotz, "Contrastive learning of medical visual representations from paired images and text," *arXiv preprint arXiv:2010.00747*, 2020.
- [393] S.-C. Huang, L. Shen, M. P. Lungren, and S. Yeung, "Gloria: A multimodal global-local representation learning framework for label-efficient medical image recognition," in *ICCV*, 2021.
- [394] H.-Y. Zhou, X. Chen, Y. Zhang, R. Luo, L. Wang, and Y. Yu, "Generalized radiograph representation learning via cross-supervision between images and free-text radiology reports," *Nature Machine Intelligence*, vol. 4, 2022.
- [395] X. Wang, Y. Ye, and A. Gupta, "Zero-shot recognition via semantic embeddings and knowledge graphs," in *CVPR*, 2018.